Numer Algor (2018) 78:569–597
DOI 10.1007/s11075-017-0389-7

ORIGINAL PAPER

An explicitly uncoupled VMS stabilization finite element method for the time-dependent Darcy-Brinkman equations in double-diffusive convection

Yun-Bo Yang[1] · **Yao-Lin Jiang**[1]

Received: 28 July 2016 / Accepted: 31 July 2017 / Published online: 23 August 2017

Abstract In this article, a full explicitly uncoupled variational multiscale (VMS) stabilization finite element method for solving the Darcy-Brinkman equations in double-diffusive convection is proposed. This method introduces three uncoupled VMS treatments for the velocity, the temperature, and the concentration as the post-processing steps at each time step, respectively. We only need first to solve three full decoupled linear problems and then to solve three full decoupled postprocessing problems. This method is easy to implement because the existing codes can be used. The unconditional stability is proved and the a priori error estimates are derived. A series of numerical experiments are also given to confirm the theoretical analysis and to demonstrate the efficiency of the new method.

Keywords Double-diffusive convection · Darcy-Brinkman · Finite element method · Variational multiscale method · Uncoupled and modular postprocessing

Mathematics Subject Classification (2010) 65N15 · 65N30 · 65N12 · 65M12

1 Introduction

The nonlinear time-dependent Darcy-Brinkman equations can describe the double-diffusion phenomena in a confined porous enclosure, and its dimensionless form is

✉ Yao-Lin Jiang
yljiang@mail.xjtu.edu.cn

Yun-Bo Yang
yangyunbo@stu.xjtu.edu.cn

[1] School of Mathematics and Statistics, Xi'an Jiaotong University, Xi'an, 710049, Shaanxi, People's Republic of China

described as following [8, 13, 30, 33]: for a bounded and regular domain $\Omega \subset \mathbb{R}^d$ ($d = 2$ or 3), given final time t_f, find $\mathbf{u} : \Omega \times [0, t_f] \to \mathbb{R}^d$, $p : \Omega \times [0, t_f] \to \mathbb{R}$, $T : \Omega \times [0, t_f] \to \mathbb{R}$, and $C : \Omega \times [0, t_f] \to \mathbb{R}$ satisfying

$$
\begin{aligned}
&\mathbf{u}_t - \nu\Delta\mathbf{u} + (\mathbf{u}\cdot\nabla)\mathbf{u} + Da^{-1}\mathbf{u} + \nabla p = (\beta_T T + \beta_C C)\mathbf{g} \quad \text{in } (0, t_f]\times\Omega,\\
&\nabla\cdot\mathbf{u} = 0 \quad \text{in } (0, t_f]\times\Omega, \mathbf{u} = 0 \ \text{ on } (0, t_f]\times\partial\Omega,\\
&T_t - \nabla\cdot(\gamma\nabla T) + (\mathbf{u}\cdot\nabla)T = 0 \ \text{ in } (0, t_f]\times\Omega,\\
&C_t - \nabla\cdot(Dc\nabla C) + (\mathbf{u}\cdot\nabla)C = 0 \ \text{ in } (0, t_f]\times\Omega,\\
&T, C = 0 \ \text{ on } \Gamma_T, \quad \frac{\partial T}{\partial\mathbf{n}} = 0, \frac{\partial C}{\partial\mathbf{n}} = 0 \ \text{ on } \Gamma_B,\\
&\mathbf{u}(0, x) = u_0, T(0, x) = T_0, C(0, x) = C_0 \text{ in } \Omega,
\end{aligned}
\tag{1}
$$

where $\mathbf{u}$ represents the velocity, p the pressure, T the temperature, C the concentration, $\mathbf{n}$ is the outward unit normal on Ω, and $\Gamma_T = \partial\Omega \setminus \Gamma_B$, where Γ_B is a regular open subset of $\partial\Omega$. Moreover, ν is the kinematic viscosity, γ is the thermal diffusivity, Dc is the mass diffusivity, Da is the Darcy number, $\mathbf{g}$ is the gravitational acceleration vector, β_T and β_C is the thermal and solutal expansion coefficients, respectively. The system (1) uses the Boussinesq approximation as governing equations. The other important dimensionless parameters are the thermal Grashof number $Gr_\mathrm{T} = \frac{g\beta_\mathrm{T}\triangle T\mathcal{H}^3}{\nu^2}$, the solutal Grashof number $Gr_\mathrm{C} = \frac{g\beta_\mathrm{T}\triangle C\mathcal{H}^3}{\nu^2}$, the buoyancy ratio $\mathcal{N} = \frac{\beta_\mathrm{C}\triangle C}{\beta_\mathrm{T}\triangle T}$, the Prandtl number $Pr = \frac{\nu}{\gamma}$, the Schmidt number $Sc = \frac{\nu}{D_c}$, the Lewis number $Le = \frac{Sc}{\mathrm{Pr}}$, the thermal Rayleigh number $Ra = Gr_\mathrm{T} Pr Da$, and the Darcy number $Da = \frac{K}{\mathcal{H}^2}$, where $\mathcal{H}$ denotes the cavity height and K is the permeability. In addition, $\triangle T$ and $\triangle C$ are the characteristics temperature and concentration differences along the enclosure, respectively.

The Darcy-Brinkman system (1) can describe the double-diffusive convection phenomena which arises from the combined heat and mass transfer in porous medium. It is mainly motivated by its importance in industrial applications, such as electrochemistry, metallurgy and geophysical model, grain storage, and contaminant transport in ground water; for more details, we can see [13, 25, 26, 30] and references therein. Therefore, the Darcy-Brinkman system (1) is very valuable in our real life, and it is of practical interest to study its numerical methods. One of the preferable methods for solving Darcy-Brinkman system is the Galerkin finite element method. However, it may exhibit global spurious oscillations [14, 24] and produce inaccurate and poor numerical solutions if we solve Darcy-Brinkman system by the standard Galerkin methods. One reason is the dominance of the convection term. To avoid this problem, some stabilization methods came into being.

The VMS methods are popular methods for the numerical simulation of turbulent flows, and they were first derived in [19]. The main idea of VMS methods is to define large scales by a projection into appropriate function subspaces. For more details, see [1, 15, 19–21]. Recently, some variants of VMS methods were proposed. For example, in [7], a projection-based VMS stabilization finite element technique for solving steady-state natural convection problem was presented. This projection-based stabilization method was also extended for the non-isothermal free convection problems

[23]. A subgrid stabilization method for incompressible magnetohydrodynamics was proposed in [3]. However, there also exists some questions of these VMS stabilization methods; one of these questions is how to introduce the VMS methods into existing legacy codes. In [22, 27], the authors derived a variant of VMS stabilization method for the Navier-Stokes equations; in this method, a separate, uncoupled, and modular postprocessing step is added at each time step, and this lead to the legacy codes that can be used. The theoretical analysis and numerical experiments have illustrated the efficiency of this postprocessing algorithm. This postprocessing method was combined with the characteristics time-stepping method for solving the Navier-Stokes equations in [6] and was used to solve the incompressible non-isothermal flows [2].

About the finite element numerical methods of the Darcy-Brinkman system (1), only a few articles study it. For example, a semidiscrete projection-based VMS-stabilized finite element method was proposed in [8, 33] that gave out a fully discrete subgrid-stabilized finite element method, and in [9], the author presented a fully discrete scheme with the linear extrapolation of convecting velocity terms. The main contribution of this work is that we extend the VMS postprocessing method to the Darcy-Brinkman system (1) and derive a full explicitly uncoupled VMS stabilization finite element method for this system. In this method, three uncoupled (postprocessing) VMS stabilization steps for the velocity, the temperature, and the concentration are introduced at each time step, respectively. We only need first to solve three full decoupled linear problems and then to solve three full decoupled postprocessing problems. This method is easy to implement because we can use the existing codes. The unconditional stability is proved, and the a priori error estimates for the velocity, the temperature, the concentration, and the pressure are derived, respectively. Comparing with the projection-based VMS stabilization finite element method [8], our method can save a large amount of computational cost and keep accuracy.

The article is organized as follows. In Section 2, we introduce some notations and preliminary results which will be used throughout this article, and also give out the numerical algorithm. The unconditional stability of the proposed method was proved in Section 3. A rigorous error analysis for the presented algorithm was discussed in Section 4. A series of numerical experiments are provided in Section 5 for verifying the accuracy and efficiency of the numerical method. In the end, the conclusions are given out.

2 Mathematical preliminaries

In this section, we aim to generalize some of the notations, definitions, and preliminary lemmas that will be frequently used in the analysis. Let $\Omega \subset \mathbb{R}^d (d = 2,3)$ be an open, bounded, convex, polygonal, or polyhedral domain with Lipschitz-continuous boundary $\partial\Omega$. We denote the inner product on $L^2(\Omega)$ or $L^2(\Omega)^{d\times d}$ by $(\cdot,\cdot)$, and the norm in $L^2(\Omega)$ and the norm in $L^\infty(\Omega)$ by $\|\cdot\|$ and $\|\cdot\|_\infty$, respectively. The space $H^k(\Omega)$ is used to represent the Sobolev space $W_2^k(\Omega)$ with norm $\|\cdot\|_k$. In addition, the vector spaces and vector functions will be indicated by boldface type letters, e.g., the spaces $\mathbf{H}^k(\Omega)$, $\mathbf{W}^{k,p}(\Omega)$, and $\mathbf{L}^p(\Omega)$ represent the vector Sobolev spaces $H^k(\Omega)^d$,

$W^{k,p}(\Omega)^d$, and $L^p(\Omega)^d$, respectively. For the given function $\phi(x,t)$ defined on the entire time interval $(0,t_f)$, we define the norms

$$\|\phi\|_{\infty,k} = \sup_{0<t<T} \|\phi(\cdot,t)\|_k, \text{ and } \|\phi\|_{m,k} = \left(\int_0^{t_f} \|\phi(\cdot,t)\|_k^m dt\right)^{1/m}.$$

The following Sobolev spaces for the velocity, the pressure, the temperature, and the concentration are introduced, respectively, by

$$\begin{aligned}
\mathbf{X} &= \mathbf{H}_0^1(\Omega) = \{\mathbf{v} \in \mathbf{H}^1(\Omega) : \mathbf{v} = 0 \text{ on } \partial\Omega\},\\
M &= L_0^2(\Omega) = \left\{q \in L^2(\Omega) : \int_\Omega q dx = 0\right\},\\
W &= \{S \in H^1(\Omega) : S = 0 \text{ on } \Gamma_T\},\\
\Psi &= \{D \in H^1(\Omega) : D = 0 \text{ on } \Gamma_T\}.
\end{aligned}$$

The space of divergence-free functions is

$$\mathbf{V} = \{\mathbf{v} \in \mathbf{X} : (q, \nabla\cdot\mathbf{v}) = 0, \forall q \in M\}.$$

Finally, the space $H^{-1}(\Omega)$, the dual space of $H_0^1(\Omega)$, is endowed with the negative norm

$$\|f\|_{-1} = \sup_{v\in H_0^1(\Omega)} \frac{|(f,v)|}{\|\nabla v\|}.$$

The weak formulation of (1) is given by: Find $(\mathbf{u}, p, T, C) \in (\mathbf{X}, M, W, \Psi)$, such that for any $(\mathbf{v}, q, S, D) \in (\mathbf{X}, Q, W, \Psi)$

$$\begin{aligned}
&(\mathbf{u}_t, \mathbf{v}) + \nu(\nabla\mathbf{u}, \nabla\mathbf{v}) + c_0(\mathbf{u}, \mathbf{u}, \mathbf{v}) + Da^{-1}(\mathbf{u}, \mathbf{v})\\
&\quad -(p, \nabla\cdot\mathbf{v}) = \beta_T(gT, \mathbf{v}) + \beta_C(gC, \mathbf{v}),\\
&(\nabla\cdot\mathbf{u}, q) = 0,
\end{aligned} \tag{2a}$$

$$(T_t, S) + \gamma(\nabla T, \nabla S) + c_1(\mathbf{u}, T, S) = 0, \tag{2b}$$

$$(C_t, D) + Dc(\nabla T, \nabla D) + c_2(\mathbf{u}, C, D) = 0, \tag{2c}$$

where the three skew-symmetric trilinear forms are defined as

$$\begin{aligned}
c_0(\mathbf{u}, \mathbf{v}, \mathbf{w}) &= \frac{1}{2}(\mathbf{u}\cdot\nabla\mathbf{v}, \mathbf{w}) - \frac{1}{2}(\mathbf{u}\cdot\nabla\mathbf{w}, \mathbf{v}), \forall \mathbf{u}, \mathbf{v}, \mathbf{w} \in \mathbf{X},\\
c_1(\mathbf{u}, T, S) &= \frac{1}{2}(\mathbf{u}\cdot\nabla T, S) - \frac{1}{2}(\mathbf{u}\cdot\nabla S, T), \forall \mathbf{u} \in \mathbf{X}, T, S \in W,\\
c_2(\mathbf{u}, C, D) &= \frac{1}{2}(\mathbf{u}\cdot\nabla C, D) - \frac{1}{2}(\mathbf{u}\cdot\nabla D, C), \forall \mathbf{u} \in \mathbf{X}, C, D \in \Psi.
\end{aligned}$$

Applying the Hölder's inequality, the interpolation theorems, the Sobolev embeddings, and the Poincaré's inequality, we can get the following bounds (see [8, 29]).

Lemma 1 *There exists constants K which depend on Ω such that the skew-symmetric trilinear forms satisfy the following bounds, for any $\mathbf{u}, \mathbf{v}, \mathbf{w} \in \mathbf{X}, T, S \in W$ and $C, D \in \Psi$*

$$
\begin{aligned}
&c_0(\mathbf{u}, \mathbf{v}, \mathbf{w}) \leq K\|\nabla\mathbf{u}\|\|\nabla\mathbf{v}\|\|\nabla\mathbf{w}\|,\\
&c_1(\mathbf{u}, T, S) \leq K\|\nabla\mathbf{u}\|\|\nabla T\|\|\nabla S\|,\\
&c_2(\mathbf{u}, C, D) \leq K\|\nabla\mathbf{u}\|\|\nabla C\|\|\nabla D\|,\\
&c_0(\mathbf{u}, \mathbf{v}, \mathbf{w}) \leq K\|\mathbf{u}\|^{\frac{1}{2}}\|\nabla\mathbf{u}\|^{\frac{1}{2}}\|\nabla\mathbf{v}\|\|\nabla\mathbf{w}\|,\\
&c_1(\mathbf{u}, T, S) \leq K\|\mathbf{u}\|^{\frac{1}{2}}\|\nabla\mathbf{u}\|^{\frac{1}{2}}\|\nabla T\|\|\nabla S\|,\\
&c_2(\mathbf{u}, C, D) \leq K\|\mathbf{u}\|^{\frac{1}{2}}\|\nabla\mathbf{u}\|^{\frac{1}{2}}\|\nabla C\|\|\nabla D\|.
\end{aligned}
$$

Next, we introduce the finite element discretization of the problem (2). Set $\tau_h = \{\Omega_h\}$ and $\tau_H = \{\Omega_H\}$ are two uniformly regular triangulation of domain Ω. Here, h (resp.H) denotes the maximum diameter of the elements in τ_h (resp.τ_H) and such that $h < H$. Let $\mathbf{X}_h \subset \mathbf{X}$, $M_h \subset M$, $W_h \subset W$, and $\Psi_h \in \Psi$ be conforming finite element spaces. We also assume that the conforming velocity-pressure finite element space $(\mathbf{X}_h, M_h) \subset (\mathbf{X}, M)$ satisfies the discrete inf-sup condition (see [16]), i.e., there exists a constant $\beta > 0$ independent of h such that

$$
\inf_{q_h \in M_h} \sup_{\mathbf{v}_h \in \mathbf{X}_h} \frac{(q_h, \nabla \cdot \mathbf{v}_h)}{\|q_h\|\|\nabla\mathbf{v}_h\|} \geq \beta > 0. \tag{3}
$$

Examples of such conforming finite element spaces are the classical Taylor-Hood element $(P_k, P_{k-1})(k \geq 2)$ (see [28]), the (P_2, P_0) element (see [10]), and the Scott-Vogelius elements $(P_k, P_{k-1}^{\text{disc}})(k \geq 2)$ on appropriate meshes (see [5]). The space of the discrete divergence-free functions is defined as

$$
\mathbf{V}_h = \{\mathbf{v}_h \in \mathbf{X}_h : (q_h, \nabla \cdot \mathbf{v}_h) = 0, \forall q_h \in M_h\}.
$$

Defining

$$
\begin{aligned}
&P_{V_h}^{L^2} : \mathbf{L}^2(\Omega) \to \mathbf{V}_h,\ P_{M_h}^{L^2} : L^2(\Omega) \to M_h,\\
&P_{W_h}^{L^2} : L^2(\Omega) \to W_h,\ P_{\Psi_h}^{L^2} : L^2(\Omega) \to \Psi_h
\end{aligned}
$$

by the L^2-orthogonal projections into $\mathbf{V}_h$, M_h, W_h, and Ψ_h, respectively, they satisfy

$$
\begin{aligned}
&(P_{V_h}^{L^2}\mathbf{v} - \mathbf{v}, \mathbf{v}_h) = 0, \forall \mathbf{v}_h \in \mathbf{V}_h,\\
&(P_{M_h}^{L^2} q - q, q_h) = 0, \forall q_h \in M_h,\\
&(P_{W_h}^{L^2} S - S, S_h) = 0, \forall S_h \in W_h,\\
&(P_{\Psi_h}^{L^2} D - D, D_h) = 0, \forall D_h \in \Psi_h.
\end{aligned}
$$

It is well known that the projections $P_{V_h}^{L^2}$, $P_{M_h}^{L^2}$, $P_{W_h}^{L^2}$, and $P_{\Psi_h}^{L^2}$ satisfy the following approximation properties (see [4, 12, 29])

$$\begin{aligned}
&\|\mathbf{u} - P_{V_h}^{L^2}\mathbf{u}\| + h\|\nabla(\mathbf{u} - P_{V_h}^{L^2}\mathbf{u})\| \le Kh^{k+1}\|\mathbf{u}\|_{k+1}, \forall \mathbf{u} \in \mathbf{V} \cup \mathbf{H}^{k+1}(\Omega),\\
&\|p - P_{M_h}^{L^2}p\| \le Kh^k\|p\|_k, \forall p \in M \cup H^k(\Omega),\\
&\|T - P_{W_h}^{L^2}T\| + h\|\nabla(T - P_{W_h}^{L^2}T)\| \le Kh^{k+1}\|T\|_{k+1}, \forall T \in W \cup H^{k+1}(\Omega),\\
&\|C - P_{\psi_h}^{L^2}C\| + h\|\nabla(C - P_{\psi_h}^{L^2}C)\| \le Kh^{k+1}\|C\|_{k+1}, \forall C \in \Psi \cup H^{k+1}(\Omega). \quad (4)
\end{aligned}$$

Let Δt be the time step size, $t_n = n\Delta t$, $n = 0, 1, 2, ..., N$, with $t_f := N\Delta t$. For notational clarity, we denote by v^n the function v evaluated at $t = t_n$, where $t_n = n\Delta t$. We also define the following additional norms:

$$|||\upsilon|||_{\infty,k} := \max_{0\le n\le N-1} \|\upsilon^{n+1}\|_k, \; |||\upsilon|||_{m,k} := \left(\sum_{n=0}^{N-1} \|\upsilon^{n+1}\|_k^m \Delta t\right)^{1/m}.$$

Moreover, we define the norms of the dual spaces of $\mathbf{X}_h$ and $\mathbf{V}_h$, respectively, by

$$\|\psi\|_{\mathbf{X}_h'} = \sup_{\mathbf{v}_h\in\mathbf{X}_h} \frac{(\psi, \mathbf{v}_h)}{\|\nabla\mathbf{v}_h\|}, \; \|\psi\|_{\mathbf{V}_h'} = \sup_{\mathbf{v}_h\in\mathbf{V}_h} \frac{(\psi, \mathbf{v}_h)}{\|\nabla\mathbf{v}_h\|}.$$

Lemma 2 [11]. *The norm $\|\mathbf{v}\|_{X_h'}$ and $\|\mathbf{v}\|_{V_h'}$ are equivalent for any $\mathbf{v} \in \mathbf{V}_h$.*

The error analysis uses a discrete Gronwall inequality, recalled from [18].

Lemma 3 *(Discrete Gronwall's Lemma). Let Δt, H and a_n, b_n, c_n, d_n (for integers $n \ge 0$) be nonnegative numbers such that*

$$a_l + \Delta t \sum_{n=0}^{l} b_n \le \Delta t \sum_{n=0}^{l-1} d_n a_n + \Delta t \sum_{n=0}^{l} c_n + H, l \ge 0,$$

then for all $\Delta t \ge 0$,

$$a_l + \Delta t \sum_{n=0}^{l} b_n \le \exp\left(\Delta t \sum_{n=0}^{l-1} d_n\right)\left(\Delta t \sum_{n=0}^{l} c_n + H\right), l \ge 0.$$

We also need assume further that the mesh is sufficiently regular such that the inverse inequality holds [4]:

$$\|\nabla\mathbf{v}_h\| \le Ch^{-1}\|\mathbf{v}_h\|, \;\; \forall \mathbf{v}_h \in \mathbf{X}_h.$$

Furthermore, the Young's and Poincar´e's inequalities as follows will be used frequently

$$\begin{aligned}
&ab \le \frac{\varepsilon}{p}a^p + \frac{\varepsilon^{-q/p}}{q}b^q, a, b, p, q, \varepsilon \in \mathbb{R}, \frac{1}{p} + \frac{1}{q} = 1, p, q \in (1, \infty), \varepsilon > 0,\\
&\|\upsilon\| \le C_p\|\nabla\upsilon\|, \forall \upsilon \in \mathbf{X} \text{ (or } W \text{or } \Psi), K_p = K_p(\Omega).
\end{aligned}$$

For stating our method, we need to introduce the coarse or large scale spaces L_H, Q_H, and G_H on the coarse mesh τ_H for the deformation tensor, the temperature gradient, and the concentration gradient, respectively, i.e. with

$$\begin{aligned} &L_H \subseteq \nabla \mathbf{X}_h \subseteq L := \{l_{ij} \in L^2(\Omega)^{d\times d} | l_{ij} = l_{ji}\}, \\ &Q_H \subseteq \nabla W_h \subseteq Q := \{q_i \in L^2(\Omega)^d\}, \\ &G_H \subseteq \nabla \Phi_h \subseteq G := \{g_i \in L^2(\Omega)^d\}. \end{aligned} \tag{5}$$

Remark 1 The choice of the coarse spaces L_H, Q_H, and G_H is very important (see [20] for a discussion of this). There are different choices of selecting L_H, Q_H, and G_H, which lead to different VMS methods. Herein, we can choose $L_H = \nabla \mathbf{X}_H$, $Q_H = \nabla W_H$, and $G_H = \nabla \Phi_H$; this is to say that L_H, Q_H, and G_H are the spaces of polynomials of degree $k-1$. Although the larger H provides for more efficient projections into L_H, Q_H, and G_H and reduces storage, it also reduces the accuracy. Thus, the choice of H must be balanced between efficiency and accuracy.

The relevant L^2 orthogonal projection operators for those coarse- or large-scale finite element spaces are defined as

$$P_u^L : L \to L_H,\ P_T^Q : Q \to Q_H,\ P_C^G : G \to G_H,$$

and they satisfy

$$\|R - P_\mu^\kappa R\| \le K H^k \|R\|_k, \mu = u, T, C;\ \kappa = L, Q, G, \tag{6}$$

for all $R \in H^k(\Omega)$.

The full explicitly uncoupled variational multiscale method for the problem (2) is given out as follows.

Algorithm 1 *(The full explicitly uncoupled VMS method) Let the time step size Δt and final time t_f are given, $N = t_f/\Delta t$, $n = 0, 1, \cdots, N-1$, $\mathbf{u}_h^0 = \hat{\mathbf{u}}_h^0 = P_{V_h}^{L^2}\mathbf{u}_0$, $T_h^0 = \hat{T}_h^0 = P_{W_h}^{L^2}T_0$, $C_h^0 = \hat{C}_h^0 = P_{\Psi_h}^{L^2}C_0$, find $(\mathbf{u}_h^{n+1}, p_h^{n+1}, T_h^{n+1}, C_h^{n+1}) \in (\mathbf{X}_h, M_h, W_h, \Psi_h)$ via the following two steps:*

Step 1: *Find $(\hat{\mathbf{u}}_h^{n+1}, p_h^{n+1}, \hat{T}_h^{n+1}, \hat{C}_h^{n+1}) \in (\mathbf{X}_h, M_h, W_h, \Psi_h)$, such that for any $(\hat{\mathbf{v}}_h, \hat{q}_h, \hat{S}_h, \hat{D}_h) \in (\mathbf{X}_h, Q_h, W_h, \Psi_h)$*

$$\begin{aligned} &\left(\frac{\hat{\mathbf{u}}_h^{n+1} - \mathbf{u}_h^n}{\Delta t}, \hat{\mathbf{v}}_h\right) + \nu(\nabla \hat{\mathbf{u}}_h^{n+1}, \nabla \hat{\mathbf{v}}_h) + c_0(\mathbf{u}_h^n, \hat{\mathbf{u}}_h^{n+1}, \hat{\mathbf{v}}_h) \\ &\quad + Da^{-1}(\hat{\mathbf{u}}_h^{n+1}, \hat{\mathbf{v}}_h) - (p_h^{n+1}, \nabla \cdot \hat{\mathbf{v}}_h) = \beta_T(\mathbf{g}T_h^n, \hat{\mathbf{v}}_h) + \beta_C(\mathbf{g}C_h^n, \hat{\mathbf{v}}_h), \\ &(\nabla \cdot \hat{\mathbf{u}}_h^{n+1}, \hat{q}_h) = 0, \end{aligned} \tag{7a}$$

$$\left(\frac{\hat{T}_h^{n+1} - T_h^n}{\Delta t}, \hat{S}_h\right) + \gamma(\nabla \hat{T}_h^{n+1}, \nabla \hat{S}_h) + c_1(\mathbf{u}_h^n, \hat{T}_h^{n+1}, \hat{S}_h) = 0, \tag{7b}$$

$$\left(\frac{\hat{C}_h^{n+1}-C_h^n}{\Delta t},\hat{D}_h\right)+Dc(\nabla\hat{C}_h^{n+1},\nabla\hat{D}_h)+c_2(\mathbf{u}_h^n,\hat{C}_h^{n+1},\hat{D}_h)=0. \tag{7c}$$

Step 2: *Find* $(\mathbf{u}_h^{n+1},T_h^{n+1},C_h^{n+1})\in(\mathbf{X}_h,W_h,\Psi_h)$, *such that for any* $(\mathbf{v}_h,q_h,S_h,D_h)\in(\mathbf{X}_h,Q_h,W_h,\Psi_h)$

$$\left(\frac{\hat{\mathbf{u}}_h^{n+1}-\mathbf{u}_h^{n+1}}{\Delta t},\mathbf{v}_h\right)=(\lambda_h^{n+1},\nabla\cdot\mathbf{v}_h)+\alpha_1(\nabla\mathbf{u}_h^{n+1},\nabla\mathbf{v}_h)-\alpha_1(P_u^L\nabla\mathbf{u}_h^n,P_u^L\nabla\mathbf{v}_h),$$

$$(\nabla\cdot\mathbf{u}_h^{n+1},q_h)=0, \tag{8a}$$

$$\left(\frac{\hat{T}_h^{n+1}-T_h^{n+1}}{\Delta t},S_h\right)=\alpha_2(\nabla T_h^{n+1},\nabla S_h)-\alpha_2(P_T^Q\nabla T_h^n,P_T^Q\nabla S_h), \tag{8b}$$

$$\left(\frac{\hat{C}_h^{n+1}-C_h^{n+1}}{\Delta t},D_h\right)=\alpha_3(\nabla C_h^{n+1},\nabla D_h)-\alpha_3(P_C^G\nabla C_h^n,P_C^G\nabla D_h). \tag{8c}$$

Remark 2 In Algorithm 1, the temperature equation and the concentration equation are decoupled from the fluid equations, and the projection steps are also decoupled; this leads to the scheme is decoupled into six sub-problems, and each sub-problem is linear. However, it is still unconditionally stable with respect to the time step size. Comparing the projection-based stabilization method [8], which is a nonlinear scheme for the Darcy-Brinkman equations in double-diffusive convection, Algorithm 1 is more effective and it can save a large amount of computational cost; numerical experiments will illustrate it.

Remark 3 The eddy viscosity stabilization parameters $\alpha_i(i=1,2,3)$ are user-defined constants; with the proper choosing of stabilized parameters, the optimal error estimates can be obtained for the velocity, the temperature, and the concentration, respectively. What is more, the extra projection terms in Step 2 are defined on the coarse-/large-scale spaces L_H, Q_H, and G_H for the velocity, temperature, and concentration. Thus, the stabilization terms in Step 2 act directly only on the small scales.

3 Stability analysis

Now, we prove the unconditional stability of Algorithm 1 which ensure the existence of the numerical solutions.

Theorem 1 *Assume that* $\mathbf{u}_0\in\mathbf{H}^1(\Omega)$, $T_0\in H^1(\Omega)$, *and* $C_0\in H^1(\Omega)$, *then Algorithm 1 is unconditionally stable, and for all* $N\geq 1$, *it satisfies the following energy estimates*

$$\begin{aligned}&\|T_h^N\|^2+\alpha_2\Delta t\|\nabla T_h^N\|^2+\alpha_2\Delta t\sum_{n=0}^{N-1}\|(I-P_T^Q)\nabla T_h^{n+1}\|^2\\&\leq\|T_0\|^2+\alpha_2\Delta t\|\nabla T_0\|^2,\end{aligned} \tag{9}$$

$$\|C_h^N\|^2 + \alpha_3\Delta t\|\nabla C_h^N\|^2 + \alpha_3\Delta t\sum_{n=0}^{N-1}\|(I - P_C^G)\nabla C_h^{n+1}\|^2$$
$$\leq \|C_0\|^2 + \alpha_3\Delta t\|\nabla C_0\|^2, \tag{10}$$

and

$$\|\mathbf{u}_h^N\|^2 + \alpha_1\Delta t\|\nabla\mathbf{u}_h^N\|^2 + \alpha_1\Delta t\sum_{n=0}^{N-1}\|(I - P_u^L)\nabla\mathbf{u}_h^{n+1}\|^2$$
$$\leq \|\mathbf{u}_0\|^2 + \alpha_1\Delta t\|\nabla\mathbf{u}_0\|^2 + 2Da\beta_T^2\|\mathbf{g}\|_\infty^2 t_f(\|T_0\|^2 + \alpha_2\Delta t\|\nabla T_0\|^2)$$
$$+2Da\beta_C^2\|\mathbf{g}\|_\infty^2 t_f(\|T_0\|^2 + \alpha_3\Delta t\|\nabla C_0\|^2). \tag{11}$$

Proof Setting $\hat{S}_h = \hat{T}_h^{n+1}$ in (7b) and $S_h = T_h^{n+1}$ in (8b), we have

$$\|\hat{T}_h^{n+1}\|^2 + \gamma\Delta t\|\nabla\hat{T}_h^{n+1}\|^2 = (T_h^n, \hat{T}_h^{n+1}),$$
$$\|T_h^{n+1}\|^2 + \alpha_2\Delta t\|\nabla T_h^{n+1}\|^2 = (\hat{T}_h^{n+1}, T_h^{n+1}) + \alpha_2\Delta t(P_T^Q\nabla T_h^n, P_T^Q\nabla T_h^{n+1}). \tag{12}$$

Making use of the Cauchy-Schwarz and Young's inequalities on the right-hand side of (12) along with the properties of orthogonal projection, we arrive at

$$\frac{1}{2}\|\hat{T}_h^{n+1}\|^2 + \gamma\Delta t\|\nabla\hat{T}_h^{n+1}\|^2 \leq \frac{1}{2}\|T_h^n\|^2, \tag{13}$$

and

$$\frac{1}{2}\|T_h^{n+1}\|^2 + \frac{\alpha_2\Delta t}{2}(\|\nabla T_h^{n+1}\|^2 - \|\nabla T_h^n\|^2) + \frac{\alpha_2\Delta t}{2}\|(I - P_T^Q)\nabla T_h^{n+1}\|^2$$
$$\leq \frac{1}{2}\|\hat{T}_h^{n+1}\|^2. \tag{14}$$

Thus,

$$\frac{1}{2}\|T_h^{n+1}\|^2 + \frac{\alpha_2\Delta t}{2}(\|\nabla T_h^{n+1}\|^2 - \|\nabla T_h^n\|^2) + \frac{\alpha_2\Delta t}{2}\|(I - P_T^Q)\nabla T_h^{n+1}\|^2$$
$$\leq \frac{1}{2}\|T_h^n\|^2. \tag{15}$$

Taking sum of (15) from $n = 1$ to $N - 1$, we get the estimate (9), and the estimate (10) can be obtained by using the analogous way. We next prove the estimate (11). From (9) and (10), we know

$$\Delta t\sum_{n=0}^{N-1}\|T_h^n\|^2 \leq t_f(\|T_h^0\|^2 + \alpha_2\Delta t\|\nabla T_h^0\|^2), \tag{16}$$

and

$$\Delta t\sum_{n=0}^{N-1}\|C_h^n\|^2 \leq t_f(\|C_h^0\|^2 + \alpha_3\Delta t\|\nabla C_h^0\|^2). \tag{17}$$

Choosing $\hat{\mathbf{v}}_h = \hat{\mathbf{u}}_h^{n+1} \in \mathbf{V}_h$ in (7a) and making use of the Cauchy-Schwarz and Young's inequalities to arrived at

$$\begin{aligned}&\frac{1}{2}\|\hat{\mathbf{u}}_h^{n+1}\|^2 + \nu\Delta t\|\nabla\hat{\mathbf{u}}_h^{n+1}\|^2 + \frac{\Delta t Da^{-1}}{2}\|\hat{\mathbf{u}}_h^{n+1}\|^2\\ &\leq \frac{1}{2}\|\mathbf{u}_h^n\|^2 + Da\beta_T^2\|\mathbf{g}\|_\infty^2\Delta t\|T_h^n\|^2 + Da\beta_C^2\|\mathbf{g}\|_\infty^2\Delta t\|C_h^n\|^2. \end{aligned} \tag{18}$$

Taking $\mathbf{v}_h = \mathbf{u}_h^{n+1} \in \mathbf{V}_h$ in (8a) and using the properties of orthogonal projection to derive

$$\begin{aligned}&\frac{1}{2}\|\mathbf{u}_h^{n+1}\|^2 + \frac{\alpha_1\Delta t}{2}(\|\nabla\mathbf{u}_h^{n+1}\|^2 - \|\nabla\mathbf{u}_h^n\|^2) + \frac{\alpha_1\Delta t}{2}\|(I - P_u^L)\nabla\mathbf{u}_h^{n+1}\|^2\\ &\leq \frac{1}{2}\|\hat{\mathbf{u}}_h^{n+1}\|^2. \end{aligned} \tag{19}$$

By (18) and (19), we get

$$\begin{aligned}&\frac{1}{2}\|\mathbf{u}_h^{n+1}\|^2 + \frac{\alpha_1\Delta t}{2}(\|\nabla\mathbf{u}_h^{n+1}\|^2 - \|\nabla\mathbf{u}_h^n\|^2) + \frac{\alpha_1\Delta t}{2}\|(I - P_u^L)\nabla\mathbf{u}_h^{n+1}\|^2\\ &\leq \frac{1}{2}\|\mathbf{u}_h^n\|^2 + Da\beta_T^2\|\mathbf{g}\|_\infty^2\Delta t\|T_h^n\|^2 + Da\beta_C^2\|\mathbf{g}\|_\infty^2\Delta t\|C_h^n\|^2. \end{aligned} \tag{20}$$

Summing (20) from $n = 0$ to $N-1$ and combining (16) and (17), we get the estimate (11) and complete the proof. □

Applying Theorem 1, we can get the bounds on $\hat{\mathbf{u}}_h$ and $\hat{T}_h$ and $\hat{C}_h$ as follows.

Theorem 2 *Under the assumptions of Theorem 1, the solution $(\hat{\mathbf{u}}_h, \hat{T}_h, \hat{C}_h)$ of Algorithm 1 satisfies the following energy estimates*

$$\|\hat{T}_h^N\|^2 + 2\gamma\Delta t\sum_{n=0}^{N-1}\|\nabla\hat{T}_h^{n+1}\|^2 \leq 2\|T_0\|^2 + \alpha_2\Delta t\|\nabla T_0\|^2, \tag{21}$$

$$\|\hat{C}_h^N\|^2 + 2Dc\Delta t\sum_{n=0}^{N-1}\|\nabla\hat{C}_h^{n+1}\|^2 \leq 2\|C_0\|^2 + \alpha_3\Delta t\|\nabla C_0\|^2, \tag{22}$$

and

$$\begin{aligned}&\|\hat{\mathbf{u}}_h^N\|^2 + 2\nu\Delta t\sum_{n=0}^{N-1}\|\nabla\hat{\mathbf{u}}_h^{n+1}\|^2 + Da^{-1}\Delta t\sum_{n=0}^{N-1}\|\hat{\mathbf{u}}_h^{n+1}\|^2\\ &\leq 2\|\mathbf{u}_0\|^2 + \alpha_1\Delta t\|\nabla\mathbf{u}_0\|^2 + 2Da\beta_T^2\|\mathbf{g}\|_\infty^2 t_f(\|T_0\|^2 + \alpha_2\Delta t\|\nabla T_0\|^2)\\ &\quad + 2Da\beta_C^2\|\mathbf{g}\|_\infty^2 t_f(\|C_0\|^2 + \alpha_3\Delta t\|\nabla C_0\|^2), \end{aligned} \tag{23}$$

Proof Summing (13) from $n = 0$ to $N-1$ and summing (14) from $n = 0$ to $N-2$ to arrive

$$\sum_{n=0}^{N-1}\|\hat{T}_h^{n+1}\|^2 + 2\gamma\Delta t\sum_{n=0}^{N-1}\|\hat{T}_h^{n+1}\|^2 \leq \sum_{n=0}^{N-1}\|T_h^n\|^2, \tag{24}$$

and

$$\sum_{n=0}^{N-2}\|T_h^{n+1}\|^2+\alpha_2\Delta t\|\nabla T_h^N\|^2+\alpha_2\Delta t\sum_{n=0}^{N-2}\|(I-P_T^Q)\nabla T_h^{n+1}\|^2$$
$$\leq \alpha_2\Delta t\|\nabla T_h^0\|^2+\sum_{n=0}^{N-2}\|\hat{T}_h^{n+1}\|^2. \tag{25}$$

Applying the identity relation $\sum_{n=0}^{N-2}a^{n+1}=\sum_{n=0}^{N-1}a^n-a^0$ in (25) and using it in (24), we have

$$\sum_{n=0}^{N-1}\|\hat{T}_h^{n+1}\|^2+2\gamma\Delta t\sum_{n=0}^{N-1}\|\hat{T}_h^{n+1}\|^2\leq\|T_h^0\|^2+\alpha_2\Delta t\|\nabla T_h^0\|^2+\sum_{n=0}^{N-1}\|\hat{T}_h^n\|^2. \tag{26}$$

Thus, we get the estimate (21), and the estimates (22) and (23) can be obtained by using the analogous way. Now, the proof is completed. □

4 Error analysis

In this section, we will give out the convergence results of Algorithm 1 for the velocity, the temperature, and the concentration in Theorem 3 and Corollary 1, and for the pressure in Theorem 4.

In order to establish the optimal asymptotic error estimates of Algorithm 1, we need to assume that the true solution of problem (2) satisfies the following regularity assumptions:

$$\begin{aligned}&\mathbf{u}\in L^\infty(0,T;\mathbf{H}^3(\Omega))\cap L^2(0,T;\mathbf{H}^{k+1}(\Omega))\\&\qquad\cap H^1(0,T;\mathbf{H}^1(\Omega))\cap H^2(0,T;\mathbf{L}^2(\Omega)),\\&T,C\in L^\infty(0,T;H^3(\Omega))\cap L^2(0,T;H^{k+1}(\Omega))\\&\qquad\cap H^1(0,T;H^1(\Omega))\cap H^2(0,T;L^2(\Omega)),\\&p\in L^2(0,T;H^k(\Omega)).\end{aligned}\tag{27}$$

Defining the following error decompositions:

$$\begin{aligned}\hat{\mathbf{e}}_u^n&=\mathbf{u}^n-\hat{\mathbf{u}}_h^n=(\mathbf{u}^n-P_{V_h}^{L^2}\mathbf{u}^n)-(\hat{\mathbf{u}}_h^n-P_{V_h}^{L^2}\mathbf{u}^n)=\eta_u^n-\hat{\phi}_u^n,\\\mathbf{e}_u^n&=\mathbf{u}^n-\mathbf{u}_h^n=(\mathbf{u}^n-P_{V_h}^{L^2}\mathbf{u}^n)-(\mathbf{u}_h^n-P_{V_h}^{L^2}\mathbf{u}^n)=\eta_u^n-\phi_u^n,\\\hat{e}_T^n&=T^n-\hat{T}_h^n=(T^n-P_{W_h}^{L^2}T^n)-(\hat{T}_h^n-P_{W_h}^{L^2}T^n)=\eta_T^n-\hat{\phi}_T^n,\\e_T^n&=T^n-T_h^n=(T^n-P_{W_h}^{L^2}T^n)-(T_h^n-P_{W_h}^{L^2}T^n)=\eta_T^n-\phi_T^n,\\\hat{e}_C^n&=C^n-\hat{C}_h^n=(C^n-P_{\Psi_h}^{L^2}C^n)-(\hat{C}_h^n-P_{\Psi_h}^{L^2}C^n)=\eta_C^n-\hat{\phi}_C^n,\\e_C^n&=C^n-C_h^n=(C^n-P_{\Psi_h}^{L^2}C^n)-(C_h^n-P_{\Psi_h}^{L^2}C^n)=\eta_C^n-\phi_C^n,\end{aligned}\tag{28}$$

where $P_{V_h}^{L^2}$, $P_{W_h}^{L^2}$, and $P_{\Psi_h}^{L^2}$ denote the L^2 orthogonal projection onto $\mathbf{V}_h$, W_h, and Ψ_h, respectively.

Theorem 3 *Assume that* $(\mathbf{u}, p, T, C)$ *are described by* (27)*, satisfying the weak form* (2)*, and* $(\mathbf{u}_h^{n+1}, T_h^{n+1}, C_h^{n+1})$ *are given by the Algorithm 1, then there exists a positive constant* K *independent of the mesh width* h *and time step size* Δt *such that the following error estimate hold*

$$\begin{aligned}
&\|\mathbf{e}_u^N\|^2 + \|e_T^N\|^2 + \|e_C^N\|^2 + \sum_{n=0}^{N-1}(\|\hat{\mathbf{e}}_u^{n+1} - \mathbf{e}_u^n\|^2 + \|\hat{\mathbf{e}}_u^{n+1} - \mathbf{e}_u^{n+1}\|^2) \\
&\quad + Da^{-1}\Delta t \sum_{n=0}^{N-1} \|\hat{\mathbf{e}}_u^{n+1}\|^2 + \Delta t \sum_{n=0}^{N-1} \Big(\nu \|\nabla \hat{\mathbf{e}}_u^{n+1}\|^2 + \gamma \|\nabla \hat{e}_T^{n+1}\|^2 \\
&\quad + Dc \|\nabla \hat{e}_C^{n+1}\|^2 + \alpha_1 \|\nabla \mathbf{e}_u^{n+1}\|^2 + \alpha_2 \|\nabla e_T^{n+1}\|^2 + \alpha_3 \|\nabla e_C^{n+1}\|^2 \Big) \\
&\quad \le K[h^{2k} + \Delta t^2 + (\alpha_1 + \alpha_2 + \alpha_3)(h^{2k} + \Delta t^2 + H^{2k})].
\end{aligned} \tag{29}$$

Proof Subtracting (7a)–(7c) from (2a)–(2c) at $t = t_{n+1}$ separately, it gives

$$\begin{aligned}
&\left(\frac{\mathbf{u}^{n+1} - \hat{\mathbf{u}}_h^{n+1} - (\mathbf{u}^n - \mathbf{u}_h^n)}{\Delta t}, \hat{\mathbf{v}}_h \right) + \nu(\nabla(\mathbf{u}^{n+1} - \hat{\mathbf{u}}_h^{n+1}), \nabla \hat{\mathbf{v}}_h) \\
&\quad + Da^{-1}(\mathbf{u}^{n+1} - \hat{\mathbf{u}}_h^{n+1}, \hat{\mathbf{v}}_h) + c_0(\mathbf{u}^{n+1}, \mathbf{u}^{n+1}, \hat{\mathbf{v}}_h) - c_0(\mathbf{u}_h^n, \hat{\mathbf{u}}_h^{n+1}, \hat{\mathbf{v}}_h) \\
&\quad - (p^{n+1} - p_h^{n+1}, \nabla \cdot \hat{\mathbf{v}}_h) \\
&= \beta_T(\mathbf{g}(T^{n+1} - T_h^n), \hat{\mathbf{v}}_h) + \beta_C(\mathbf{g}(C^{n+1} - C_h^n), \hat{\mathbf{v}}_h) \\
&\quad + \left(\frac{\mathbf{u}^{n+1} - \mathbf{u}^n}{\Delta t} - \mathbf{u}_t(t_{n+1}), \hat{\mathbf{v}}_h \right),
\end{aligned} \tag{30}$$

for any $(\hat{\mathbf{v}}_h, q_h) \in (\mathbf{X}_h, M_h)$,

$$\begin{aligned}
&\left(\frac{T^{n+1} - \hat{T}_h^{n+1} - (T^n - T_h^n)}{\Delta t}, \hat{S}_h \right) + \gamma(\nabla(T^{n+1} - \hat{T}_h^{n+1}), \nabla \hat{S}_h) \\
&\quad + c_1(\mathbf{u}^{n+1}, T^{n+1}, \hat{S}_h) - c_1(\mathbf{u}_h^n, \hat{T}_h^{n+1}, \hat{S}_h) \\
&= \left(\frac{T^{n+1} - T^n}{\Delta t} - T_t(t_{n+1}), \hat{S}_h \right),
\end{aligned} \tag{31}$$

for any $\hat{S}_h \in W_h$ and

$$\begin{aligned}
&\left(\frac{C^{n+1} - \hat{C}_h^{n+1} - (C^n - C_h^n)}{\Delta t}, \hat{D}_h \right) + Dc(\nabla(C^{n+1} - \hat{C}_h^{n+1}), \nabla \hat{D}_h) \\
&\quad + c_2(\mathbf{u}^{n+1}, C^{n+1}, \hat{D}_h) - c_1(\mathbf{u}_h^n, \hat{C}_h^{n+1}, \hat{D}_h) \\
&= \left(\frac{C^{n+1} - C^n}{\Delta t} - C_t(t_{n+1}), \hat{D}_h \right),
\end{aligned} \tag{32}$$

for any $\hat{D}_h \in \Psi_h$.

Setting $\hat{\mathbf{v}}_h = \hat{\phi}_u^{n+1} \in \mathbf{V}_h$ in (30). Due to the orthogonality of L^2 projection operator $P_{V_h}^{L^2}$, that $\eta_u^{n+1} - \eta_u^n \perp \mathbf{V}_h$, so $\frac{1}{\Delta t}(\eta_u^{n+1} - \eta_u^n, \hat{\phi}_u^{n+1}) = 0$, then we have

$$\begin{aligned}
&\frac{1}{2\Delta t}(\|\hat{\phi}_u^{n+1}\|^2 - \|\phi_u^n\|^2) + \frac{1}{2\Delta t}\|\hat{\phi}_u^{n+1} - \phi_u^n\|^2 + \nu\|\nabla\hat{\phi}_u^{n+1}\|^2 + Da^{-1}\|\hat{\phi}_u^{n+1}\|^2 \\
&= (\nabla\eta_u^{n+1}, \nabla\hat{\phi}_u^{n+1}) + Da^{-1}(\eta_u^{n+1}, \hat{\phi}_u^{n+1}) + c_0(\mathbf{u}^{n+1}, \mathbf{u}^{n+1}, \hat{\phi}_u^{n+1}) \\
&\quad - c_0(\mathbf{u}_h^n, \hat{\mathbf{u}}_h^{n+1}, \hat{\phi}_u^{n+1}) - (p^{n+1} - q_h, \nabla\cdot\hat{\phi}_u^{n+1}) - \beta_T(\mathbf{g}(T^{n+1} - T^n), \hat{\phi}_u^{n+1}) \\
&\quad - \beta_T(\mathbf{g}\eta_T^n, \hat{\phi}_u^{n+1}) + \beta_T(\mathbf{g}\phi_T^n, \hat{\phi}_u^{n+1}) - \beta_C(\mathbf{g}(C^{n+1} - C^n), \hat{\phi}_u^{n+1}) \\
&\quad - \beta_C(\mathbf{g}\eta_C^n, \hat{\phi}_u^{n+1}) + \beta_C(\mathbf{g}\phi_C^n, \hat{\phi}_u^{n+1}) - \left(\frac{\mathbf{u}^{n+1} - \mathbf{u}^n}{\Delta t} - \mathbf{u}_t(t_{n+1}), \hat{\phi}_u^{n+1}\right). \quad (33)
\end{aligned}$$

Choosing $\mathbf{v}_h = \phi_u^{n+1} \in \mathbf{V}_h$ in (8a), we have

$$\left(\frac{\hat{\mathbf{u}}_h^{n+1} - \mathbf{u}_h^{n+1}}{\Delta t}, \phi_u^{n+1}\right) = \alpha_1(\nabla\mathbf{u}_h^{n+1}, \nabla\phi_u^{n+1}) - \alpha_1(P_u^L\nabla\mathbf{u}_h^n, P_u^L\nabla\phi_u^{n+1}). \quad (34)$$

Noting that

$$\begin{aligned}
\mathrm{LHS}_{(34)} &= \left(\frac{\hat{\mathbf{u}}_h^{n+1} - \mathbf{u}^{n+1} + \mathbf{u}^{n+1} - \mathbf{u}_h^{n+1}}{\Delta t}, \phi_u^{n+1}\right) \\
&= \frac{1}{\Delta t}(\hat{\phi}_u^{n+1} - \phi_u^{n+1}, \phi_u^{n+1}) \\
&= \frac{1}{2\Delta t}(\|\hat{\phi}_u^{n+1}\|^2 - \|\phi_u^{n+1}\|^2 - \|\hat{\phi}_u^{n+1} - \phi_u^{n+1}\|^2), \quad (35)
\end{aligned}$$

and

$$\begin{aligned}
\mathrm{RHS}_{(34)} &= \alpha_1(\nabla\mathbf{u}_h^{n+1}, \nabla\phi_u^{n+1}) - \alpha_1(P_u^L\nabla\mathbf{u}_h^n, P_u^L\nabla\phi_u^{n+1}) \\
&\quad - \alpha_1(P_u^L\nabla\mathbf{u}_h^n, (I - P_u^L)\nabla\phi_u^{n+1}) \\
&= \alpha_1(\nabla\mathbf{u}_h^{n+1}, \nabla\phi_u^{n+1}) - \alpha_1(P_u^L\nabla\mathbf{u}_h^n, \nabla\phi_u^{n+1}) \\
&= \alpha_1(\nabla(\mathbf{u}_h^{n+1} - \mathbf{u}^{n+1} + \mathbf{u}^{n+1} - \mathbf{u}^n + \mathbf{u}^n - P_u^L\mathbf{u}^n \\
&\qquad + P_u^L\mathbf{u}^n - P_u^L\mathbf{u}_h^n), \nabla\phi_u^{n+1}) \\
&= -\alpha_1(\nabla\eta_u^{n+1}, \nabla\phi_u^{n+1}) + \alpha_1\|\nabla\phi_u^{n+1}\|^2 \\
&\quad + \alpha_1(\nabla(\mathbf{u}^{n+1} - \mathbf{u}^n), \nabla\phi_u^{n+1}) + \alpha_1(\nabla(\mathbf{u}^n - P_u^L\mathbf{u}^n), \nabla\phi_u^{n+1}) \\
&\quad + \alpha_1(\nabla P_u^L\eta_u^n, \nabla\phi_u^{n+1}) - \alpha_1(\nabla P_u^L\phi_u^n, \nabla\phi_u^{n+1}). \quad (36)
\end{aligned}$$

Then, combining (33)–(36), we get the momentum error equation as follows:

$$\begin{aligned}
&\frac{1}{2\Delta t}(\|\phi_u^{n+1}\|^2 - \|\phi_u^n\|^2) + \frac{1}{2\Delta t}(\|\hat{\phi}_u^{n+1} - \phi_u^n\|^2 + \|\hat{\phi}_u^{n+1} - \phi_u^{n+1}\|^2) \\
&\quad + \nu\|\nabla\hat{\phi}_u^{n+1}\|^2 + Da^{-1}\|\hat{\phi}_u^{n+1}\|^2 + \alpha_1\|\nabla\phi_u^{n+1}\|^2 \\
&= \nu(\nabla\eta_u^{n+1}, \nabla\hat{\phi}_u^{n+1}) + Da^{-1}(\eta_u^{n+1}, \hat{\phi}_u^{n+1}) + c_0(\mathbf{u}^{n+1}, \mathbf{u}^{n+1}, \hat{\phi}_u^{n+1})
\end{aligned}$$

$$
\begin{aligned}
&-c_0(\mathbf{u}_h^n, \hat{\mathbf{u}}_h^{n+1}, \hat{\phi}_u^{n+1}) - (p^{n+1} - q_h, \nabla \cdot \hat{\phi}_u^{n+1}) - \beta_{\mathrm{T}}(\mathbf{g}(T^{n+1} - T^n), \hat{\phi}_u^{n+1}) \\
&-\beta_{\mathrm{T}}(\mathbf{g}\eta_{\mathrm{T}}^n, \hat{\phi}_u^{n+1}) + \beta_{\mathrm{T}}(\mathbf{g}\phi_{\mathrm{T}}^n, \hat{\phi}_u^{n+1}) - \beta_{\mathrm{C}}(\mathbf{g}(C^{n+1} - C^n), \hat{\phi}_u^{n+1}) \\
&-\beta_{\mathrm{C}}(\mathbf{g}\eta_{\mathrm{C}}^n, \hat{\phi}_u^{n+1}) + \beta_{\mathrm{C}}(\mathbf{g}\phi_{\mathrm{C}}^n, \hat{\phi}_u^{n+1}) - \left(\frac{\mathbf{u}^{n+1} - \mathbf{u}^n}{\Delta t} - \mathbf{u}_t(t_{n+1}), \hat{\phi}_u^{n+1}\right) \\
&+\alpha_1(\nabla\eta_u^{n+1}, \nabla\phi_u^{n+1}) - \alpha_1(\nabla(\mathbf{u}^{n+1} - \mathbf{u}^n), \nabla\phi_u^{n+1}) - \alpha_1(\nabla P_u^L\eta_u^n, \nabla\phi_u^{n+1}) \\
&-\alpha_1(\nabla(\mathbf{u}^n - P_u^L\mathbf{u}^n), \nabla\phi_u^{n+1}) + \alpha_1(\nabla P_u^L\phi_u^n, \nabla\phi_u^{n+1}). \qquad (37)
\end{aligned}
$$

By using the same techniques, we can get the temperature error equation as

$$
\begin{aligned}
&\frac{1}{2\Delta t}(\|\phi_T^{n+1}\|^2 - \|\phi_T^n\|^2) + \frac{1}{2\Delta t}(\|\hat{\phi}_T^{n+1} - \phi_T^n\|^2 + \|\hat{\phi}_T^{n+1} - \phi_T^{n+1}\|^2) \\
&\quad +\gamma\|\nabla\hat{\phi}_T^{n+1}\|^2 + \alpha_2\|\nabla\phi_T^{n+1}\|^2 \\
&= \gamma(\nabla\eta_T^{n+1}, \nabla\hat{\phi}_T^{n+1}) + c_1(\mathbf{u}^{n+1}, T^{n+1}, \hat{\phi}_T^{n+1}) - c_1(\mathbf{u}_h^n, \hat{T}_h^{n+1}, \hat{\phi}_T^{n+1}) \\
&\quad -\left(\frac{T^{n+1} - T^n}{\Delta t} - T_t(t_{n+1}), \hat{\phi}_T^{n+1}\right) + \alpha_2(\nabla\eta_T^{n+1}, \nabla\phi_T^{n+1}) \\
&\quad -\alpha_2(\nabla(T^{n+1} - T^n), \nabla\phi_T^{n+1}) - \alpha_2(\nabla(T^n - P_T^Q T^n), \nabla\phi_T^{n+1}) \\
&\quad -\alpha_2(\nabla P_u^Q\eta_T^n, \nabla\phi_T^{n+1}) + \alpha_2(\nabla P_T^Q\phi_T^n, \nabla\phi_T^{n+1}). \qquad (38)
\end{aligned}
$$

and the concentration error equation as

$$
\begin{aligned}
&\frac{1}{2\Delta t}(\|\phi_C^{n+1}\|^2 - \|\phi_C^n\|^2) + \frac{1}{2\Delta t}(\|\hat{\phi}_C^{n+1} - \phi_C^n\|^2 + \|\hat{\phi}_C^{n+1} - \phi_C^{n+1}\|^2) \\
&\quad +Dc\|\nabla\hat{\phi}_C^{n+1}\|^2 + \alpha_3\|\nabla\phi_3^{n+1}\|^2 \\
&= Dc(\nabla\eta_C^{n+1}, \nabla\hat{\phi}_C^{n+1}) + c_2(\mathbf{u}^{n+1}, C^{n+1}, \hat{\phi}_C^{n+1}) - c_2(\mathbf{u}_h^n, \hat{C}_h^{n+1}, \hat{\phi}_C^{n+1}) \\
&\quad -\left(\frac{C^{n+1} - C^n}{\Delta t} - C_t(t_{n+1}), \hat{\phi}_C^{n+1}\right) + \alpha_3(\nabla\eta_C^{n+1}, \nabla\phi_C^{n+1}) \\
&\quad -\alpha_3(\nabla(C^{n+1} - C^n), \nabla\phi_C^{n+1}) - \alpha_3(\nabla(C^n - P_C^G C^n), \nabla\phi_C^{n+1}) \\
&\quad -\alpha_3(\nabla P_C^G\eta_C^n, \nabla\phi_C^{n+1}) + \alpha_3(\nabla P_C^G\phi_C^n, \nabla\phi_C^{n+1}). \qquad (39)
\end{aligned}
$$

Next, we estimate the terms on the right-hand side of the momentum error equation (37) as follows. The first two terms can be bounded by using the Cauchy-Schwarz and Young's inequalities as follows:

$$
\nu(\nabla\eta_u^{n+1}, \nabla\hat{\phi}_u^{n+1}) \le \frac{\nu}{14}\|\nabla\hat{\phi}_u^{n+1}\|^2 + K\nu\|\nabla\eta_u^{n+1}\|^2, \qquad (40)
$$

$$
Da^{-1}(\eta_u^{n+1}, \hat{\phi}_u^{n+1}) \le \frac{Da^{-1}}{14}\|\hat{\phi}_u^{n+1}\|^2 + K\,Da\|\eta_u^{n+1}\|^2. \qquad (41)
$$

Noticing that the following identity hold

$$\begin{aligned}
&c_0(\mathbf{u}^{n+1},\mathbf{u}^{n+1},\hat{\mathbf{v}}_h)-c_0(\mathbf{u}_h^n,\hat{\mathbf{u}}_h^{n+1},\hat{\mathbf{v}}_h)\\
&=c_0(\mathbf{u}^{n+1}-\mathbf{u}^n,\mathbf{u}^{n+1},\hat{\mathbf{v}}_h)+c_0(\eta_u^n,\mathbf{u}^{n+1},\hat{\mathbf{v}}_h)-c_0(\phi_u^n,P_{V_h}^{L^2}\mathbf{u}^{n+1},\hat{\mathbf{v}}_h)\\
&\quad+c_0(P_{V_h}^{L^2}\mathbf{u}^n,\eta_u^{n+1},\hat{\mathbf{v}}_h)-c_0(P_{V_h}^{L^2}\mathbf{u}^n,\hat{\phi}_u^{n+1},\hat{\mathbf{v}}_h)-c_0(\phi_u^n,\hat{\phi}_u^{n+1},\hat{\mathbf{v}}_h)\\
&=\sum_{i=1}^{6}\Lambda_{hi}(\hat{\mathbf{v}}_h).
\end{aligned}\tag{42}$$

Due to skew symmetry of the trilinear form, we know $\Lambda_{h5}(\hat{\phi}_u^{n+1})=0$ and $\Lambda_{h6}(\hat{\phi}_u^{n+1})=0$. Using Lemma 1, the Sobolev embedding and the Young's inequality to get

$$\begin{aligned}
\Lambda_{h1}(\hat{\phi}_u^{n+1}) &\le K\|\nabla(\mathbf{u}^{n+1}-\mathbf{u}^n)\|\|\nabla\mathbf{u}^{n+1}\|\|\nabla\hat{\phi}_u^{n+1}\|\\
&\le \frac{\nu}{14}\|\nabla\hat{\phi}_u^{n+1}\|^2+\frac{K}{\nu}\|\nabla\mathbf{u}^{n+1}\|^2\Delta t\int_{t_n}^{t_{n+1}}\|\nabla\mathbf{u}_t\|^2dt,
\end{aligned}\tag{43}$$

$$\begin{aligned}
\Lambda_{h2}(\hat{\phi}_u^{n+1}) &\le K\|\nabla\eta_u^n\|\|\nabla\mathbf{u}^{n+1}\|\|\nabla\hat{\phi}_u^{n+1}\|\\
&\le \frac{\nu}{14}\|\nabla\hat{\phi}_u^{n+1}\|^2+\frac{K}{\nu}\|\nabla\mathbf{u}^{n+1}\|^2\|\nabla\eta_u^n\|^2,
\end{aligned}\tag{44}$$

$$\begin{aligned}
\Lambda_{h3}(\hat{\phi}_u^{n+1}) &\le K\|\phi_u^n\|(\|P_{V_h}^{L^2}\mathbf{u}^{n+1}\|_{L^\infty}+\|P_{V_h}^{L^2}\nabla\mathbf{u}^{n+1}\|_{L^3})\|\nabla\hat{\phi}_u^{n+1}\|\\
&\le \frac{\nu}{14}\|\nabla\hat{\phi}_u^{n+1}\|^2+\frac{K}{\nu}\|\mathbf{u}^{n+1}\|_2^2\|\phi_u^n\|^2,
\end{aligned}\tag{45}$$

and

$$\begin{aligned}
\Lambda_{h4}(\hat{\phi}_u^{n+1}) &\le K\|\nabla P_{V_h}^{L^2}\mathbf{u}^n\|\|\nabla\eta_u^{n+1}\|\|\nabla\hat{\phi}_u^{n+1}\|\\
&\le \frac{\nu}{14}\|\nabla\hat{\phi}_u^{n+1}\|^2+\frac{K}{\nu}\|\nabla\mathbf{u}^n\|^2\|\nabla\eta_u^{n+1}\|^2.
\end{aligned}\tag{46}$$

For the remaining terms, we have

$$\begin{aligned}
(p^{n+1}-q_h,\nabla\cdot\hat{\phi}_u^{n+1}) &\le \sqrt{d}\|\nabla\hat{\phi}_u^{n+1}\|\|p^{n+1}-q_h\|\\
&\le \frac{\nu}{14}\|\nabla\hat{\phi}_u^{n+1}\|^2+\frac{K}{\nu}\|p^{n+1}-q_h\|^2,
\end{aligned}\tag{47}$$

$$\begin{aligned}
&\beta_{\mathrm{T}}(\mathbf{g}(T^{n+1}-T^n),\hat{\phi}_u^{n+1})\\
&\le \beta_{\mathrm{T}}\|\mathbf{g}\|_\infty\|T^{n+1}-T^n\|\|\hat{\phi}_u^{n+1}\|\\
&\le \frac{Da^{-1}}{14}\|\hat{\phi}_u^{n+1}\|^2+KDa\beta_{\mathrm{T}}^2\|\mathbf{g}\|_\infty^2\Delta t\int_{t_n}^{t_{n+1}}\|T_t\|^2dt,
\end{aligned}\tag{48}$$

$$\beta_{\mathrm{T}}(\mathbf{g}\eta_T^n,\hat{\phi}_u^{n+1})\le\frac{Da^{-1}}{14}\|\hat{\phi}_u^{n+1}\|^2+KDa\beta_{\mathrm{T}}^2\|\mathbf{g}\|_\infty^2\|\eta_T^n\|^2,\tag{49}$$

$$\beta_{\mathrm{T}}(\mathbf{g}\phi_T^n,\hat{\phi}_u^{n+1})\le\frac{Da^{-1}}{14}\|\hat{\phi}_u^{n+1}\|^2+KDa\beta_{\mathrm{T}}^2\|\mathbf{g}\|_\infty^2\|\phi_T^n\|^2,\tag{50}$$

$$\begin{aligned}&\beta_{\mathrm{C}}(\mathbf{g}(C^{n+1}-C^n),\hat{\phi}_u^{n+1})\\&\le \frac{Da^{-1}}{14}\|\hat{\phi}_u^{n+1}\|^2+K\,Da\beta_{\mathrm{C}}^2\|\mathbf{g}\|_\infty^2\Delta t\int_{t_n}^{t_{n+1}}\|C_t\|^2dt,\end{aligned}\tag{51}$$

$$\beta_{\mathrm{C}}(\mathbf{g}\eta_C^n,\hat{\phi}_u^{n+1})\le\frac{Da^{-1}}{14}\|\hat{\phi}_u^{n+1}\|^2+K\,Da\beta_{\mathrm{C}}^2\|\mathbf{g}\|_\infty^2\|\eta_C^n\|^2,\tag{52}$$

$$\beta_{\mathrm{C}}(\mathbf{g}\phi_C^n,\hat{\phi}_u^{n+1})\le\frac{Da^{-1}}{14}\|\hat{\phi}_u^{n+1}\|^2+K\,Da\beta_{\mathrm{C}}^2\|\mathbf{g}\|_\infty^2\|\phi_C^n\|^2,\tag{53}$$

$$\begin{aligned}\left(\frac{\mathbf{u}^{n+1}-\mathbf{u}^n}{\Delta t}-\mathbf{u}_t(t_{n+1}),\hat{\phi}_u^{n+1}\right)&\le K_p\|\frac{\mathbf{u}^{n+1}-\mathbf{u}^n}{\Delta t}-\mathbf{u}_t(t_{n+1})\|\|\hat{\phi}_u^{n+1}\|\\&\le\frac{\nu}{14}\|\nabla\hat{\phi}_u^{n+1}\|^2+\frac{K}{\nu}\Delta t\int_{t_n}^{t_{n+1}}\|\mathbf{u}_{tt}\|^2dt.\end{aligned}\tag{54}$$

For the last five terms on the right-hand side of (37), we can estimate them by the usual way as follows:

$$\begin{aligned}&\alpha_1(\nabla\eta_u^{n+1},\nabla\phi_u^{n+1})\le\frac{\alpha_1}{10}\|\nabla\phi_u^{n+1}\|^2+K\alpha_1\|\nabla\eta_u^{n+1}\|^2,\\&\alpha_1(\nabla(\mathbf{u}^{n+1}-\mathbf{u}^n),\nabla\phi_u^{n+1})\le\frac{\alpha_1}{10}\|\nabla\phi_u^{n+1}\|^2+K\alpha_1\Delta t\int_{t_n}^{t_{n+1}}\|\nabla\mathbf{u}_t\|^2dt,\\&\alpha_1(\nabla(\mathbf{u}^n-P_u^L\mathbf{u}^n),\nabla\phi_u^{n+1})\le\frac{\alpha_1}{10}\|\nabla\phi_u^{n+1}\|^2+K\alpha_1\|\nabla(\mathbf{u}^n-P_u^L\mathbf{u}^n)\|^2,\\&\alpha_1(\nabla P_u^L\eta_u^n,\nabla\phi_u^{n+1})\le\frac{\alpha_1}{10}\|\nabla\phi_u^{n+1}\|^2+K\alpha_1\|\nabla\eta_u^n\|^2,\\&\alpha_1(\nabla P_u^L\phi_u^n,\nabla\phi_u^{n+1})\le\frac{\alpha_1}{10}\|\nabla\phi_u^{n+1}\|^2+K\alpha_1h^{-2}\|\phi_u^n\|^2.\end{aligned}\tag{55}$$

Combining estimates (40)–(55), and regrouping terms, the momentum error equation (37) becomes

$$\begin{aligned}&\frac{1}{2\Delta t}(\|\phi_u^{n+1}\|^2-\|\phi_u^n\|^2)+\frac{1}{2\Delta t}(\|\hat{\phi}_u^{n+1}-\phi_u^n\|^2+\|\hat{\phi}_u^{n+1}-\phi_u^{n+1}\|^2)\\&\quad+\frac{\nu}{2}\|\nabla\hat{\phi}_u^{n+1}\|^2+\frac{Da^{-1}}{2}\|\hat{\phi}_u^{n+1}\|^2+\frac{\alpha_1}{2}\|\nabla\phi_u^{n+1}\|^2\\&\le K\left(\frac{1}{\nu}\|\mathbf{u}^{n+1}\|_2^2+\alpha_1h^{-2}\right)\|\phi_u^n\|^2+K\,Da\beta_{\mathrm{T}}^2\|\mathbf{g}\|_\infty^2\|\phi_T^n\|^2\\&\quad+K\,Da\beta_{\mathrm{C}}^2\|\mathbf{g}\|_\infty^2\|\phi_C^n\|^2+K\nu\|\nabla\eta_u^{n+1}\|^2+K\,Da\|\eta_u^{n+1}\|^2\\&\quad+\frac{K}{\nu}\|p^{n+1}-q_h\|^2+\frac{K}{\nu}(\|\nabla\mathbf{u}^{n+1}\|^2\|\nabla\eta_u^n\|^2+\|\nabla\mathbf{u}^n\|^2\|\nabla\eta_u^{n+1}\|^2)\\&\quad+\frac{K}{\nu}\|\nabla\mathbf{u}^{n+1}\|^2\Delta t\int_{t_n}^{t_{n+1}}\|\nabla\mathbf{u}_t\|^2dt+K\,Da\beta_{\mathrm{T}}^2\|\mathbf{g}\|_\infty^2\Delta t\int_{t_n}^{t_{n+1}}\|T_t\|^2dt\\&\quad+K\,Da\beta_{\mathrm{T}}^2\|\mathbf{g}\|_\infty^2\|\eta_T^n\|^2+K\,Da\beta_{\mathrm{C}}^2\|\mathbf{g}\|_\infty^2\|\eta_C^n\|^2+\frac{K}{\nu}\Delta t\int_{t_n}^{t_{n+1}}\|\mathbf{u}_{tt}\|^2dt\end{aligned}$$

$$+K\,Da\beta_{\mathrm{C}}^2\|\mathbf{g}\|_\infty^2\Delta t\int_{t_n}^{t_{n+1}}\|C_t\|^2dt+K\alpha_1\Delta t\int_{t_n}^{t_{n+1}}\|\nabla\mathbf{u}_t\|^2dt$$
$$+K\alpha_1\|\nabla\eta_u^{n+1}\|^2+K\alpha_1\|\nabla(\mathbf{u}^n-P_u^L\mathbf{u}^n)\|^2+K\alpha_1\|\nabla\eta_u^n\|^2. \tag{56}$$

Multiplying through by $2\Delta t$ and taking the sum from $n=0$ to $N-1$ for (56), and using the approximation properties (4) and (6), it gives

$$\begin{aligned}
&\|\phi_u^N\|^2+\sum_{n=0}^{N-1}(\|\hat{\phi}_u^{n+1}-\phi_u^n\|^2+\|\hat{\phi}_u^{n+1}-\phi_u^{n+1}\|^2)+\nu\Delta t\sum_{n=0}^{N-1}\|\nabla\hat{\phi}_u^{n+1}\|^2\\
&\quad+Da^{-1}\Delta t\sum_{n=0}^{N-1}\|\hat{\phi}_u^{n+1}\|^2+\alpha_1\Delta t\sum_{n=0}^{N-1}\|\nabla\phi_u^{n+1}\|^2\\
&\le K\Delta t\sum_{n=0}^{N-1}\left(\frac{1}{\nu}\||\mathbf{u}\||_{\infty,2}^2+\alpha_1h^{-2}\right)\|\phi_u^n\|^2+K\,Da\beta_{\mathrm{T}}^2\|\mathbf{g}\|_\infty^2\Delta t\sum_{n=0}^{N-1}\|\phi_T^n\|^2\\
&\quad+K\,Da\beta_{\mathrm{C}}^2\|\mathbf{g}\|_\infty^2\Delta t\sum_{n=0}^{N-1}\|\phi_C^n\|^2+K\nu h^{2k}\||\mathbf{u}\||_{2,k+1}^2\\
&\quad+K\,Dah^{2k+2}\||\mathbf{u}\||_{2,k+1}^2+\frac{K}{\nu}h^k\||p\||_{2,k+1}^2+\frac{K}{\nu}h^{2k}\||\mathbf{u}\||_{\infty,1}^2\||\mathbf{u}\||_{2,k+1}^2\\
&\quad+\frac{K}{\nu}\||\mathbf{u}\||_{\infty,1}^2\Delta t^2\||\mathbf{u}_t\||_{2,1}^2+K\,Da\beta_T^2\|\mathbf{g}\|_\infty^2\Delta t^2\||T_t\||_{2,0}^2\\
&\quad+K\,Da\beta_{\mathrm{T}}^2\|\mathbf{g}\|_\infty^2h^{2k+2}\||T\||_{2,k+1}^2+K\,Da\beta_{\mathrm{C}}^2\|\mathbf{g}\|_\infty^2\Delta t^2\||C_t\||_{2,0}^2\\
&\quad+K\,Da\beta_{\mathrm{C}}^2\|\mathbf{g}\|_\infty^2h^{2k+2}\||C\||_{2,k+1}^2+\frac{K}{\nu}\Delta t^2\||\mathbf{u}_{tt}\||_{2,0}^2\\
&\quad+K\alpha_1(h^{2k}\||\mathbf{u}\||_{2,k+1}^2+\Delta t^2\||\mathbf{u}_t\||_{2,1}^2+H^{2k}\||\mathbf{u}\||_{2,k+1}^2).
\end{aligned}\tag{57}$$

By using the analogous way, we get the temperature and concentration error inequalities as follows:

$$\begin{aligned}
&\|\phi_T^N\|^2+\sum_{n=0}^{N-1}(\|\hat{\phi}_T^{n+1}-\phi_T^n\|^2+\|\hat{\phi}_T^{n+1}-\phi_T^{n+1}\|^2)\\
&\quad+\gamma\Delta t\sum_{n=0}^{N-1}\|\nabla\hat{\phi}_T^{n+1}\|^2+\alpha_2\Delta t\sum_{n=0}^{N-1}\|\nabla\phi_T^{n+1}\|^2\\
&\le\frac{K}{\gamma}\Delta t\sum_{n=0}^{N-1}\||T\||_{\infty,2}^2\|\phi_u^n\|^2+\alpha_2h^{-2}\Delta t\sum_{n=0}^{N-1}\|\phi_T^n\|^2+K\gamma h^{2k}\||T\||_{2,k+1}^2\\
&\quad+\frac{K}{\gamma}h^{2k}\||T\||_{\infty,1}^2\||\mathbf{u}\||_{2,k+1}^2+\frac{K}{\gamma}\||\mathbf{u}\||_{\infty,1}^2h^{2k}\||T\||_{2,k+1}^2\\
&\quad+\frac{K}{\gamma}\||T\||_{\infty,1}^2\Delta t^2\||\mathbf{u}_t\||_{2,1}^2+\frac{K}{\gamma}\Delta t^2\||T_{tt}\||_{2,0}^2\\
&\quad+K\alpha_2(h^{2k}\||T\||_{2,k+1}^2+\Delta t^2\||T_t\||_{2,1}^2+H^{2k}\||T\||_{2,k+1}^2),
\end{aligned}\tag{58}$$

and

$$\begin{aligned}
&\|\phi_C^N\|^2 + \sum_{n=0}^{N-1}(\|\hat{\phi}_C^{n+1} - \phi_C^n\|^2 + \|\hat{\phi}_C^{n+1} - \phi_C^{n+1}\|^2) \\
&\quad + Dc\Delta t \sum_{n=0}^{N-1} \|\nabla\hat{\phi}_C^{n+1}\|^2 + \alpha_3\Delta t \sum_{n=0}^{N-1} \|\nabla\phi_C^{n+1}\|^2 \\
&\leq \frac{K}{Dc}\Delta t \sum_{n=0}^{N-1} \||C\||_{\infty,2}^2 \|\phi_u^n\|^2 + \alpha_3 h^{-2}\Delta t \sum_{n=0}^{N-1} \|\phi_C^n\|^2 + KDch^{2k}\||C\||_{2,k+1}^2 \\
&\quad + \frac{K}{Dc}h^{2k}\||C\||_{\infty,1}^2\||\mathbf{u}\||_{2,k+1}^2 + \frac{K}{Dc}\||\mathbf{u}\||_{\infty,1}^2 h^{2k}\||C\||_{2,k+1}^2 \\
&\quad + \frac{K}{Dc}\||C\||_{\infty,1}^2\Delta t^2\||\mathbf{u}_t\||_{2,1}^2 + \frac{K}{Dc}\Delta t^2\||C_{tt}\||_{2,0}^2 \\
&\quad + K\alpha_3(h^{2k}\||C\||_{2,k+1}^2 + \Delta t^2\||C_t\||_{2,1}^2 + H^{2k}\||C\||_{2,k+1}^2). \qquad (59)
\end{aligned}$$

Defining the constant

$$\begin{aligned}
\bar{d} \;=\; \max\Bigg\{ &\frac{1}{\nu}\||\mathbf{u}\||_{\infty,2}^2 + \alpha_1 h^{-2} + \frac{1}{\gamma}\||T\||_{\infty,2}^2 \\
&+ \frac{1}{Dc}\||C\||_{\infty,2}^2,\, Da\beta_{\mathrm{T}}^2\|\mathbf{g}\|_\infty^2 + \alpha_2 h^{-2},\, Da\beta_{\mathrm{C}}^2\|\mathbf{g}\|_\infty^2 + \alpha_3 h^{-2}\Bigg\}.
\end{aligned}$$

Now, adding (57), (58), and (59), dropping out some nonnegative terms, and using the discrete Gronwall Lemma, we arrive at

$$\begin{aligned}
&\|\phi_u^N\|^2 + \|\phi_T^N\|^2 + \|\phi_C^N\|^2 + \sum_{n=0}^{N-1}(\|\hat{\phi}_u^{n+1} - \phi_u^n\|^2 + \|\hat{\phi}_u^{n+1} - \phi_u^{n+1}\|^2) \\
&\quad + Da^{-1}\Delta t \sum_{n=0}^{N-1} \|\hat{\phi}_u^{n+1}\|^2 + \Delta t \sum_{n=0}^{N-1} \Big(\nu\|\nabla\hat{\phi}_u^{n+1}\|^2 + \gamma\|\nabla\hat{\phi}_T^{n+1}\|^2 \\
&\quad + Dc\|\nabla\hat{\phi}_C^{n+1}\|^2 + \alpha_1\|\nabla\phi_u^{n+1}\|^2 + \alpha_2\|\nabla\phi_T^{n+1}\|^2 + \alpha_3\|\nabla\phi_C^{n+1}\|^2\Big) \\
&\leq \exp(Kt_f\bar{d})\Bigg[\nu h^{2k}\||\mathbf{u}\||_{2,k+1}^2 + Dah^{2k+2}\||\mathbf{u}\||_{2,k+1}^2 + \frac{1}{\nu}h^{2k}\||\mathbf{u}\||_{\infty,1}^2\||\mathbf{u}\||_{2,k+1}^2 \\
&\quad + \frac{1}{\nu}\||\mathbf{u}\||_{\infty,1}^2\Delta t^2\||\mathbf{u}_t\||_{2,1}^2 + Da\beta_{\mathrm{T}}^2\|\mathbf{g}\|_\infty^2\Delta t^2\||T_t\||_{2,0}^2 + \frac{1}{\nu}h^k\||p\||_{2,k}^2 \\
&\quad + Da\beta_{\mathrm{C}}^2\|\mathbf{g}\|_\infty^2\Delta t^2\||C_t\||_{2,0}^2 + Da\beta_{\mathrm{T}}^2\|\mathbf{g}\|_\infty^2 h^{2k+2}\||T\||_{2,k+1}^2 \\
&\quad + Da\beta_{\mathrm{C}}^2\|\mathbf{g}\|_\infty^2 h^{2k+2}\||C\||_{2,k+1}^2 + \frac{1}{\gamma}\||T\||_{\infty,1}^2\Delta t^2\||\mathbf{u}_t\||_{2,1}^2 \\
&\quad + \frac{1}{\nu}\Delta t^2\||\mathbf{u}_{tt}\||_{2,0}^2 + \alpha_1(h^{2k}\||\mathbf{u}\||_{2,k+1}^2 + \Delta t^2\||\mathbf{u}_t\||_{2,1}^2 + H^{2k}\||\mathbf{u}\||_{2,k+1}^2) \\
&\quad + \frac{\Delta t^2}{\gamma}\||T_{tt}\||_{2,0}^2 + \frac{1}{\gamma}h^{2k}\|T\|_{\infty,1}^2\||\mathbf{u}\||_{2,k+1}^2 + \frac{1}{\gamma}\||u\||_{\infty,1}^2 h^{2k}\||T\||_{2,k+1}^2
\end{aligned}$$

$$+\gamma h^{2k}\||T\||^2_{2,k+1} + \alpha_2(h^{2k}\||T\||^2_{2,k+1} + \Delta t^2\||T_t\||^2_{2,1} + H^{2k}\||T\||^2_{2,k+1})$$
$$+Dch^{2k}\||C\||^2_{2,k+1} + \frac{\Delta t^2}{Dc}\||C_{tt}\||^2_{2,0} + \frac{1}{Dc}h^{2k}\|C\|^2_{\infty,1}\||\mathbf{u}\||^2_{2,k+1}$$
$$+\frac{1}{Dc}\||\mathbf{u}\||^2_{\infty,1}h^{2k}\||C\||^2_{2,k+1} + \frac{1}{Dc}\||C\||^2_{\infty,1}\Delta t^2\||\mathbf{u}_t\||^2_{2,1}$$
$$+\alpha_3(h^{2k}\||C\||^2_{2,k+1} + \Delta t^2\||C_t\||^2_{2,1} + H^{2k}\||C\||^2_{2,k+1})\Big]. \tag{60}$$

Using the regularity assumption (27) and absorbing constants into K, we get

$$\|\phi_u^N\|^2 + \|\phi_T^N\|^2 + \|\phi_C^N\|^2 + \sum_{n=0}^{N-1}(\|\hat{\phi}_u^{n+1} - \phi_u^n\|^2 + \|\hat{\phi}_u^{n+1} - \phi_u^{n+1}\|^2)$$
$$+Da^{-1}\Delta t\sum_{n=0}^{N-1}\|\hat{\phi}_u^{n+1}\|^2 + \Delta t\sum_{n=0}^{N-1}\Big(\nu\|\nabla\hat{\phi}_u^{n+1}\|^2 + \gamma\|\nabla\hat{\phi}_T^{n+1}\|^2$$
$$+Dc\|\nabla\hat{\phi}_C^{n+1}\|^2 + \alpha_1\|\nabla\phi_u^{n+1}\|^2 + \alpha_2\|\nabla\phi_T^{n+1}\|^2 + \alpha_3\|\nabla\phi_C^{n+1}\|^2\Big)$$
$$\le K[h^{2k} + \Delta t^2 + (\alpha_1 + \alpha_2 + \alpha_3)(h^{2k} + \Delta t^2 + H^{2k})]. \tag{61}$$

Applying the triangle inequality, we obtain the error estimate (29) and complete the proof. □

Corollary 1 *Under the assumptions of Theorem 3, set the eddy viscosity stabilization parameters $\alpha_i = \mathcal{O}(h^2)$, $i = 1, 2, 3$, and the coarse mesh width $H = \mathcal{O}(h^{\frac{2k-2}{2k}})$, then there exists a positive constant K such that*

$$\|\mathbf{e}_u^N\|^2 + \|e_T^N\|^2 + \|e_C^N\|^2 + \sum_{n=0}^{N-1}(\|\hat{\mathbf{e}}_u^{n+1} - \mathbf{e}_u^n\|^2 + \|\hat{\mathbf{e}}_u^{n+1} - \mathbf{e}_u^{n+1}\|^2)$$
$$+Da^{-1}\Delta t\sum_{n=0}^{N-1}\|\hat{\mathbf{e}}_u^{n+1}\|^2 + \Delta t\sum_{n=0}^{N-1}\Big(\nu\|\nabla\hat{\mathbf{e}}_u^{n+1}\|^2 + \gamma\|\nabla\hat{e}_T^{n+1}\|^2$$
$$+Dc\|\nabla\hat{e}_C^{n+1}\|^2 + \alpha_1\|\nabla\mathbf{e}_u^{n+1}\|^2 + \alpha_2\|\nabla e_T^{n+1}\|^2 + \alpha_3\|\nabla e_C^{n+1}\|^2\Big)$$
$$\le K(h^{2k} + \Delta t^2). \tag{62}$$

Remark 4 From Corollary 1, we see that Algorithm 1 can yield the accuracy of $\mathcal{O}(\Delta t + h^2)$ by using $(\mathbf{P}_2, P_1, P_2, P_2)$ finite element pair to approximate the velocity, pressure, temperature, and concentration. And we find $H = \mathcal{O}(\sqrt{h})$ is the maximum such H.

Theorem 4 *Under the same assumptions of Corollary 1, we obtain the estimate for the pressure*

$$\||p - p_h\||_{2,0} \le K(h^k + \Delta t). \tag{63}$$

Proof From (30), we have for any $\hat{\mathbf{v}}_h \in \mathbf{V}_h$ that

$$\begin{aligned}
&\left(\frac{\hat{\mathbf{e}}_u^{n+1}-\mathbf{e}_u^n}{\Delta t},\hat{\mathbf{v}}_h\right)+\nu(\nabla\hat{\mathbf{e}}_u^{n+1},\nabla\hat{\mathbf{v}}_h)+Da^{-1}(\hat{\mathbf{e}}_u^{n+1},\hat{\mathbf{v}}_h)+\sum_{i=1}^{6}\Lambda_{hi}(\hat{\mathbf{v}}_h)\\
&\quad-(p^{n+1}-\lambda_h,\nabla\cdot\hat{\mathbf{v}}_h)\\
&=\beta_{\mathrm{T}}(\mathbf{g}(T^{n+1}-T^n),\hat{\mathbf{v}}_h)+\beta_{\mathrm{T}}(\mathbf{g}e_T^n,\hat{\mathbf{v}}_h)+\beta_C(\mathbf{g}(C^{n+1}-C^n),\hat{\mathbf{v}}_h)\\
&\quad+\beta_{\mathrm{C}}(\mathbf{g}e_C^n,\hat{\mathbf{v}}_h)+\left(\frac{\mathbf{u}^{n+1}-\mathbf{u}^n}{\Delta t}-\mathbf{u}_t(t_{n+1}),\hat{\mathbf{v}}_h\right),
\end{aligned}\tag{64}$$

which together with the Cauchy-Schwarz and Poincaré inequalities yields

$$\begin{aligned}
\frac{1}{\Delta t}\frac{(\hat{\mathbf{e}}_u^{n+1}-\mathbf{e}_u^n,\hat{v}_h)}{\|\nabla\hat{\mathbf{v}}_h\|}\le K\Bigg(&\|\nabla\hat{\mathbf{e}}_u^{n+1}\|+\|\hat{\mathbf{e}}_u^{n+1}\|+\sum_{i=1}^{6}\|\Lambda_{hi}\|_{\mathbf{V}_h'}\\
&+\|p^{n+1}-\lambda_h\|+\|T^{n+1}-T^n\|+\|C^{n+1}-C^n\|\\
&+\|e_T^n\|+\|e_C^n\|+\|\frac{\mathbf{u}^{n+1}-\mathbf{u}^n}{\Delta t}-\mathbf{u}_t\,(t_{n+1}\|\Bigg).
\end{aligned}\tag{65}$$

Taking the supremum over $\hat{\mathbf{v}}_h \in \mathbf{V}_h$ and applying Lemma 2, we obtain

$$\begin{aligned}
\frac{1}{\Delta t}\|\hat{\mathbf{e}}_u^{n+1}-\mathbf{e}_u^n\|_{\mathbf{X}_h'}\le K\Bigg(&\|\nabla\hat{\mathbf{e}}_u^{n+1}\|+\|\hat{\mathbf{e}}_u^{n+1}\|+\sum_{i=1}^{6}\|\Lambda_{hi}\|_{\mathbf{X}_h'}\\
&+\|p^{n+1}-\lambda_h\|+\|T^{n+1}-T^n\|+\|C^{n+1}-C^n\|\\
&+\|e_T^n\|+\|e_C^n\|+\|\frac{\mathbf{u}^{n+1}-\mathbf{u}^n}{\Delta t}-\mathbf{u}_t(t_{n+1}\|\Bigg).
\end{aligned}\tag{66}$$

Splitting $p^{n+1}-p_h^{n+1}=(p^{n+1}-\lambda_h)+(\lambda_h-p_h^{n+1})$, where $\lambda_h\in M_h$, using (30) and the inf-sup condition (3), we have

$$\begin{aligned}
\beta\|\lambda_h-p_h^{n+1}\|&\le\sup_{\hat{\mathbf{v}}_h\in\mathbf{X}_h}\frac{(\lambda_h-p_h^{n+1},\nabla\cdot\hat{\mathbf{v}}_h)}{\|\nabla\hat{\mathbf{v}}_h\|}\\
&\le K\Bigg(\frac{1}{\Delta t}\|\hat{\mathbf{e}}_u^{n+1}-\mathbf{e}_u^n\|_{\mathbf{X}_h'}+\|\nabla\hat{\mathbf{e}}_u^{n+1}\|+\|\hat{\mathbf{e}}_u^{n+1}\|\\
&\quad+\sum_{i=1}^{6}\|\Lambda_{hi}\|_{\mathbf{X}_h'}+\|p^{n+1}-\lambda_h\|+\|T^{n+1}-T^n\|+\|e_T^n\|\\
&\quad+\|C^{n+1}-C^n\|+\|e_C^n\|+\|\frac{\mathbf{u}^{n+1}-\mathbf{u}^n}{\Delta t}-\mathbf{u}_t(t_{n+1})\|\Bigg)\\
&\le K\Bigg(\|\nabla\hat{\mathbf{e}}_u^{n+1}\|+\|\hat{\mathbf{e}}_u^{n+1}\|+\sum_{i=1}^{6}\|\Lambda_{hi}\|_{\mathbf{X}_h'}+\|p^{n+1}-\lambda_h\|\\
&\quad+\|T^{n+1}-T^n\|+\|e_T^n\|+\|C^{n+1}-C^n\|\\
&\quad+\|e_C^n\|+\|\frac{\mathbf{u}^{n+1}-\mathbf{u}^n}{\Delta t}-\mathbf{u}_t(t_{n+1})\|\Bigg).
\end{aligned}\tag{67}$$

Using the Hölder inequality and the Sobolev inequalities, we get

$$\begin{aligned}
&\Lambda_{h1}(\hat{\mathbf{v}}_h) \le K\| \int_{t_n}^{t_{n+1}} \nabla \mathbf{u}_t dt\| \|\nabla \hat{\mathbf{v}}_h\| \le K\Delta t^{\frac{1}{2}} \|\nabla \hat{\mathbf{v}}_h\|,\\
&\Lambda_{h2}(\hat{\mathbf{v}}_h) \le K h^k \|\mathbf{u}^n\|_{k+1} \|\nabla \mathbf{u}^{n+1}\| \|\nabla \hat{\mathbf{v}}_h\| \le K h^k \|\nabla \hat{\mathbf{v}}_h\|,\\
&\Lambda_{h3}(\hat{\mathbf{v}}_h) \le K \|\phi_u^n\| \|\nabla \hat{\mathbf{v}}_h\|,\\
&\Lambda_{h4}(\hat{\mathbf{v}}_h) \le K h^k \|\nabla \hat{\mathbf{v}}_h\|,\\
&\Lambda_{h5}(\hat{\mathbf{v}}_h) \le K \|\nabla \hat{\phi}_u^{n+1}\| \|\nabla \hat{\mathbf{v}}_h\|.
\end{aligned} \tag{68}$$

Noticing that by the inverse inequality and (61), we know

$$\|\nabla \phi_u^n\| \le c_{\text{inv}} h^{-1}(\Delta t + h^k) \le c^*,$$

where c^* is a constant. Thus,

$$\Lambda_{h6}(\hat{\mathbf{v}}_h) \le K \|\nabla \phi_u^n\| \|\nabla \hat{\phi}_u^{n+1}\| \|\nabla \hat{\mathbf{v}}_h\| \le K \|\nabla \hat{\phi}_u^{n+1}\| \|\nabla \hat{\mathbf{v}}_h\|. \tag{69}$$

From the estimates (68) and (69), we have

$$\sum_{i=1}^{6} \|\Lambda_{hi}\|_{\mathbf{X}_h'} \le K \left(\Delta t^{\frac{1}{2}} + h^k + \|\phi_u^n\| + \|\nabla \hat{\phi}_u^{n+1}\| \right). \tag{70}$$

Combining (70) into (67) and applying the triangle inequality yields

$$\begin{aligned}
\|p^{n+1} - p_h^{n+1}\| \le K \Big(&\|\nabla \hat{\mathbf{e}}_u^{n+1}\| + \|\hat{\mathbf{e}}_u^{n+1}\| + \Delta t^{\frac{1}{2}} + h^k + \|\phi_u^n\| \\
&+ \|\nabla \hat{\phi}_u^{n+1}\| + \|p^{n+1} - \lambda_h\| + \|T^{n+1} - T^n\| + \|e_T^n\| \\
&+ \|C^{n+1} - C^n\| + \|e_C^n\| + \|\frac{\mathbf{u}^{n+1} - \mathbf{u}^n}{\Delta t} - \mathbf{u}_t(t_{n+1})\| \Big).
\end{aligned} \tag{71}$$

With the above estimate, we have

$$\begin{aligned}
&\Delta t \sum_{n=0}^{N-1} \|p^{n+1} - p_h^{n+1}\|^2 \\
&\le K \Bigg(\Delta t \sum_{n=0}^{N-1} \|\nabla \hat{\mathbf{e}}_u^{n+1}\|^2 + \Delta t \sum_{n=0}^{N-1} \|\hat{\mathbf{e}}_u^{n+1}\|^2 + \Delta t^2 + h^{2k} \\
&\quad + \Delta t \sum_{n=0}^{N-1} \|\phi_u^n\|^2 + \Delta t \sum_{n=0}^{N-1} \|\nabla \hat{\phi}_u^{n+1}\|^2 + h^{2k} \||p\||_{2,k}^2 + \Delta t^2 \||T_t\||_{2,0}^2 \\
&\quad + \Delta t \sum_{n=0}^{N-1} \|e_T^n\|^2 + \Delta t \sum_{n=0}^{N-1} \|e_C^n\|^2 + \Delta t^2 \||\mathbf{u}_{tt}\||_{2,0}^2 \Bigg).
\end{aligned} \tag{72}$$

Now, we obtain estimate (63) by Corollary 1 and (61). □

5 Numerical experiments

In this section, we present some numerical examples to test the convergence rate and stability of the full explicitly uncoupled VMS stabilization method. Here, we choose a ($\mathbf{P}_2$, P_1, P_2, P_2) finite element pair to approximate the velocity, the pressure, the temperature, and the concentration, respectively. All the numerics were implemented by using the public domain finite element software package Freefem++ (see [17]). All computations are carried out in the domain $\Omega = [0, 1] \times [0, 1]$ and the domain Ω is subdivided into triangles.

The numerical tests are divided into two parts. We first test a problem with known analytical solution to verify the predicted convergence rates of the presented method. And next, we simulate the porous cavity problem and compare the numerical results with some benchmark dates. In all cases, the proposed method performs very effective.

5.1 Convergence rate verification

In the first test, we set the parameters $\nu = 1.0$, $Da = 1.0$, $\gamma = 1.0$, $Dc = 1.0$, $\beta_{\mathrm{T}} = 1.0$, and $\beta_{\mathrm{C}} = 1.0$. We add functions on the right-hand side of the problem (1). The boundary values of ($\mathbf{u}$, p, T, C) are given so that problem (1) has the following analytical solution

$$\begin{aligned} u_1 &= 10x^2(x-1)^2y(y-1)(2y-1)\cos(t), \\ u_2 &= -10x(x-1)(2x-1)y^2(y-1)^2\cos(t), \\ p &= 10(2x-1)(2y-1)\cos(t), \\ T &= u_1 + u_2, C = u_1 - u_2, \end{aligned}$$

where $\mathbf{u} = (u_1, u_2)$. It is easy to know that the analytical solution of the velocity is divergence-free. The initial condition is the interpolant of the true solution at $t = 0$. Set the eddy viscosity parameters $\alpha_i = h^2$, $i = 1, 2, 3$, the coarse mesh width $H = \mathcal{O}(\sqrt{h})$. We compute with the final time $t_f = 1$ and the time step size $\Delta t = h^2$, and the mesh width h is set for a refinement, each of h gets cut in a half. The convergence rates are calculated from the errors at two successive values of h in the usual manner by postulating that $E(h) = Ch^r$ and solving the formula

$$\text{Rate} = \frac{\log(E(h_i)/E(h_{i+1}))}{\log\,(h_i/h_{i+1})},$$

where $E(h_i)$ and $E(h_{i+1})$ are the errors corresponding to the mesh size h_i and h_{i+1}, respectively.

The numerical results of the full explicitly uncoupled VMS stabilization method are shown in Table 1. We can see that our method can get a quadratic convergence rate for the computed velocity, temperature and concentration in the H^1 semi-norm, and for the pressure in the L^2 norm, which verify the theoretical results. Moreover, it is easy to see that a cubic convergence rate both for the computed velocity, temperature, and concentration in the L^2 norm is obtained, which indicates that our error estimate

Table 1 Rates of convergence by using the full explicitly uncoupled VMS stabilization method with $\Delta t = h^2$, $H = \sqrt{h}$, $t_f = 1$

$\frac{1}{h}$	$\|\|\mathbf{u} - \mathbf{u}_h\|\|_{\infty,0}$	Rate	$\|\|\|\mathbf{u} - \mathbf{u}_h\|\|\|_{2,1}$	Rate	$\|\|\|p - p_h\|\|\|_{2,0}$	Rate	$\|\|T - T_h\|\|_{\infty,0}$	Rate
4	0.00196604		0.0417718		0.135942		0.00121879	
9	0.000137481	3.28055	0.00865071	1.9417	0.0271136	1.98808	8.79903e-005	3.2412
16	2.37527e-005	3.05161	0.00278116	1.97227	0.00859392	1.99696	1.5097e-005	3.06367
25	6.2204e-006	3.00225	0.00114564	1.98729	0.0035232	1.99801	3.95201e-006	3.00316
36	2.11693e-006	2.95595	0.000553877	1.99312	0.00171005	1.98234	1.33699e-006	2.97223
$\frac{1}{h}$	$\|\|\|T - T_h\|\|\|_{2,1}$	Rate	$\|\|C - C_h\|\|_{\infty,0}$	Rate	$\|\|\|C - C_h\|\|\|_{2,1}$	Rate	CPU(s)	
4	0.0256881		0.00260801		0.0523946		1.981	
9	0.00518953	1.97228	0.000173836	3.33966	0.0110446	1.91985	58.179	
16	0.00166319	1.97772	2.99983e-005	3.05367	0.00356199	1.96679	555.05	
25	0.000684794	1.98834	7.83021e-006	3.00961	0.00146801	1.98618	14224	
36	0.000330942	1.99421	2.62618e-006	2.99597	0.000709628	1.99352	16833.2	

in the L^2 norm is suboptimal. We also give out the numerical results of the projection-based VMS stabilization method [8] in Table 2. Comparing Tables 1 and 2, we can come to the conclusion that the full explicitly uncoupled VMS stabilization method can save 95.35, 94.42, 94.43, 73.48, and 83.42% CPU time when the mesh size $h = \frac{1}{4}, \frac{1}{9}, \frac{1}{16}, \frac{1}{25}, \frac{1}{36}$, respectively, and keep its accuracy.

5.2 The porous cavity problem

A classical rectangular computational domain with an aspect ratio of $A = \mathcal{H}/L$ is used. We test the case $A = 1$. The domain with its boundary conditions is illustrated in Fig. 1. We impose no-slip boundary conditions for the velocity. The horizontal

Table 2 Rates of convergence by using the projection-based VMS stabilization method [8] with $\Delta t = h^2$, $H = \sqrt{h}$, $t_f = 1$

$\frac{1}{h}$	$\|\|\mathbf{u} - \mathbf{u}_h\|\|_{\infty,0}$	Rate	$\|\|\|\mathbf{u} - \mathbf{u}_h\|\|\|_{2,1}$	Rate	$\|\|\|p - p_h\|\|\|_{2,0}$	Rate	$\|\|T - T_h\|\|_{\infty,0}$	Rate
4	0.00170756		0.0400734		0.136364		0.000985761	
9	0.00013549	3.12471	0.00862154	1.89468	0.0271169	1.99175	8.52964e-005	3.01787
16	2.36796e-005	3.03161	0.00278039	1.96688	0.00859399	1.99716	1.50139e-005	3.01923
25	6.25149e-006	2.98417	0.00114557	1.98680	0.00352188	1.99887	3.93906e-006	2.99814
36	2.1039e-006	2.98651	0.00056014	1.96210	0.0017000	1.99625	1.3295e-006	2.97862
$\frac{1}{h}$	$\|\|\|T - T_h\|\|\|_{2,1}$	Rate	$\|\|C - C_h\|\|_{\infty,0}$	Rate	$\|\|\|C - C_h\|\|\|_{2,1}$	Rate	CPU(s)	
4	0.0233561		0.00221606		0.0503984		42.558	
9	0.00514868	1.86467	0.000172489	3.14842	0.0110167	1.87507	1041.8	
16	0.00166211	1.9651	2.99614e-005	3.04229	0.00356128	1.96274	10949.3	
25	0.000684763	1.9870	7.82165e-006	3.00931	0.00146799	1.98577	53628.1	
36	0.00033335	1.97421	2.6249e-006	2.99426	0.00070866	1.99724	101490.6	

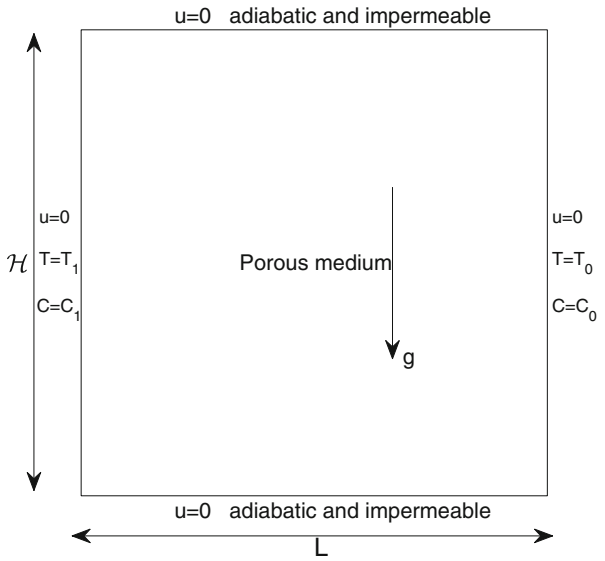

Fig. 1 The schematic diagram of the computational domain with its boundary conditions

walls are adiabatic and impermeable, and they are endowed with $\partial T/\partial n = 0$ and $\partial C/\partial n = 0$. The temperature and concentration are kept at T_0, C_0 for right and T_1, C_1 for left vertical walls with $T_0 < T_1$ and $C_0 < C_1$, respectively. We take $T_0 = C_0 = -1$ and $T_1 = C_1 = 1$.

The dimensionless Nusselt and Sherwood numbers can reflect the heat and mass transfer properties along the vertical walls and thus are important in engineering applications. In our study, the average Nusselt number and the average Sherwood number are defined as

$$Nu = \int_0^1 \left(\frac{\partial T}{\partial x}\right)_{x=0} dy, \; Su = \int_0^1 \left(\frac{\partial C}{\partial x}\right)_{x=0} dy.$$

Table 3 Comparison of the average Nusselt and Sherwood numbers for $\mathcal{N} = 0$, $Le = 10$ at $A = 1$ with different thermal Rayleigh numbers

Ra		100	200	400	1000	2000
Nu	Present	3.25	5.16	7.94	14.05	20.11
	[8]	3.15	5.02	7.83	14.01	20.00
	[13]	3.11	4.96	7.77	13.47	19.90
	[30]	3.27	5.61	9.69	–	–
Sh	Present	14.06	21.13	29.07	47.81	70.28
	[8]	13.54	20.11	27.96	48.01	71.25
	[13]	13.25	19.86	28.41	48.32	69.29
	[30]	15.61	23.23	30.73	–	–

We perform our computations for different thermal Rayleigh number Ra and implement the proposed method with the mesh width $h = \frac{1}{24}$. The values of the average Nusselt and Sherwood numbers at $A = 1$ for different thermal Rayleigh number Ra in Darcy regimes are given in Table 3, we also summarize these results along with the results obtained by Çıbık and Kaya [8], Goyeau et al. [13], and Trevisan and Bejan [30]. It show that the results are consistent with the benchmark solutions in the bibliography [8, 13, 30].

We next test the case of $\mathcal{N} = 0$ with $\beta_C = 0$, which is a purely thermal natural convection in a porous cavity. In Fig. 2, we draw the isotherm and isoconcentration lines and the streamline for $Da = 10^{-3}$, $Pr = 10$, and $Le = 10$, $A = 1$ at Ra=100, 400, and 1000, respectively. It may be seen from the results that these graphics are perfectly agreement with the ones in the investigations of [8, 13, 30] for Darcy regime even with coarser grids.

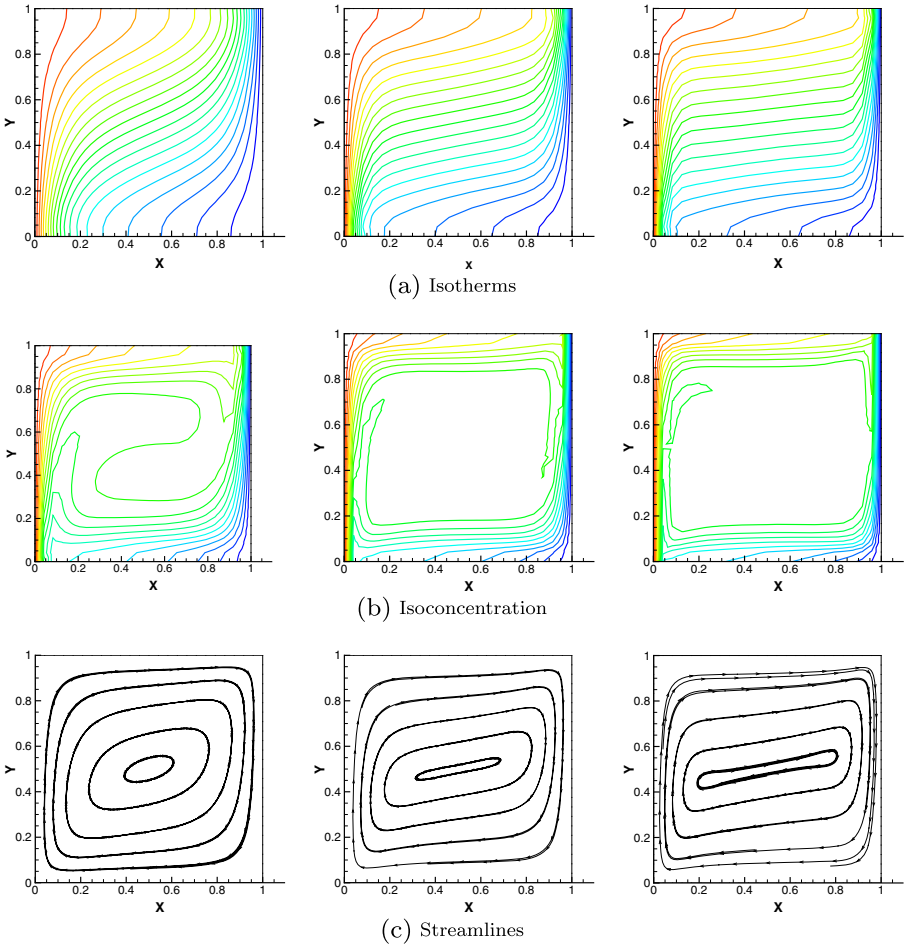

Fig. 2 Isotherm lines, isoconcentration lines, and streamline for $Da = 10^{-3}, \mathcal{N} = 0, Le = 10, A = 1$ at Ra=100, 400, and 1000 from *left* to *right*

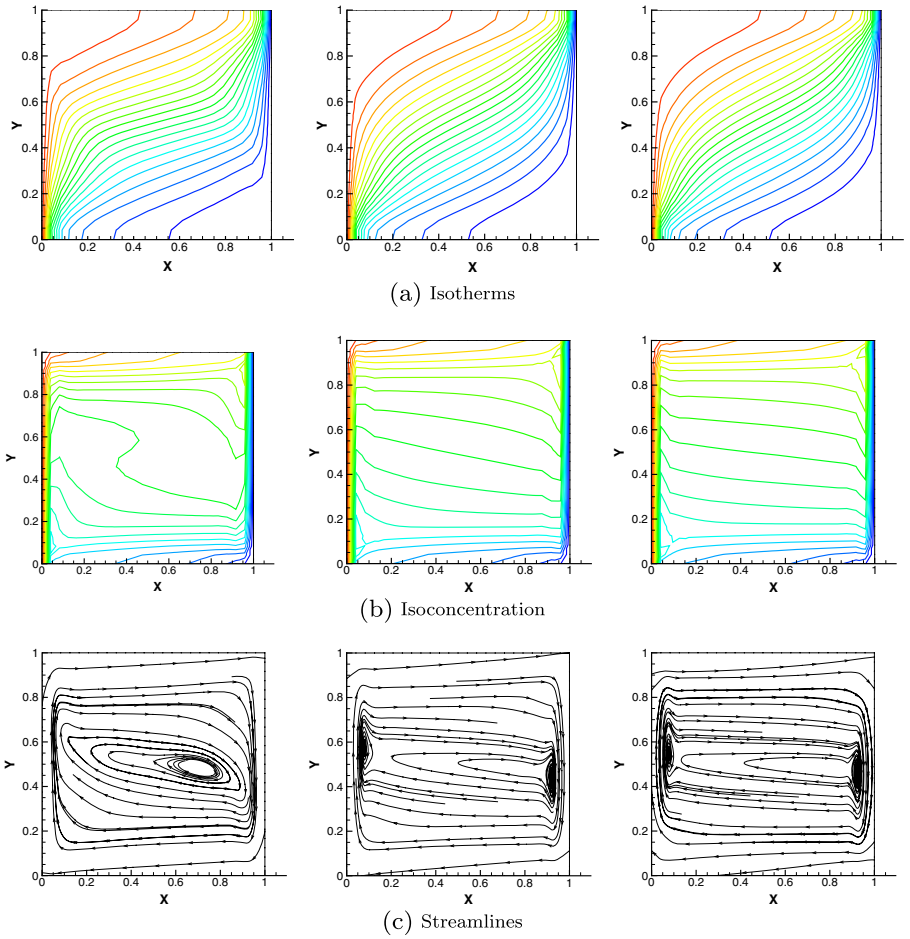

Fig. 3 Isotherm lines, isoconcentration lines and streamline for $Da = 10^{-3}$, $Ra = 400$, $Le = 10$, $A = 1$ at $\mathcal{N} = 5, 10, 15$ from *left* to *right*

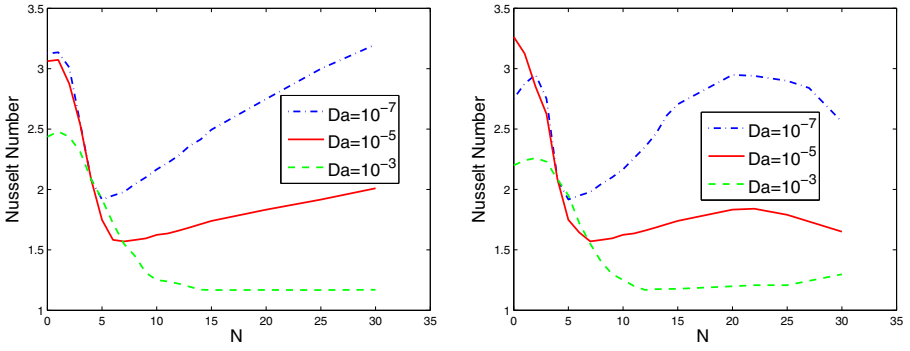

Fig. 4 The Nusselt number as a function of $\mathcal{N}$ with vary Darcy numbers solved by the present method (*left*) and the GFEM (*right*)

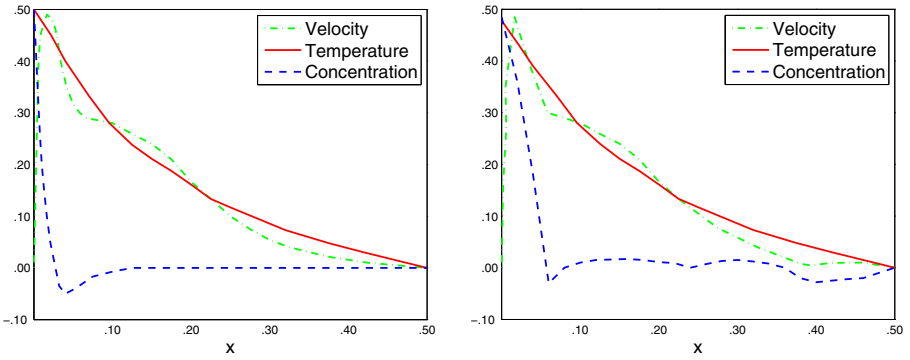

Fig. 5 The vertical velocity, temperature and concentration profiles in the horizontal midplane for $Da = 10^{-3}$, $Ra = 100$, $Le = 100$, $A = 1$ solved by the present method (*left*) and the GFEM (*right*)

We also test the case of $\mathcal{N} \neq 0$, which is identified as mass driven flow by [30] in the flow configuration. Figure 3 presents the isotherm and isoconcentration lines and the streamlines for $Da = 10^{-3}$, $Pr = 10$, Ra=400, and $Le = 10$, $A = 1$ at $\mathcal{N}$=5, 10, and 15, respectively. We can see that there are only minor changes in the isotherm with the increase of the buoyancy ratio $\mathcal{N}$, while the contour lines of the isoconcentration gradually transform into horizontal. From the streamline patterns, we can see that the circular vortex at the cavity begin to break up into two vortices tending to be close to the left and right walls. These graphics show that the concentration diffusion becomes increasingly dominant with the increase of the buoyancy ratio $\mathcal{N}$. Finally, in order to see the effect of the stabilization, we show the Nusselt number as a function of $\mathcal{N}$ with vary Darcy numbers solved by the present method and the Galerkin finite element method (GFEM) in Fig. 4. Also, we draw the horizontal midplane for the vertical velocity, temperature, and concentration profiles in Fig. 5. Those are in good agreement with the previous studies in [8, 13, 30].

6 Conclusions

In this article, we propose a full explicitly decoupled VMS stabilization method for solving the Darcy-Brinkman equations in double-diffusive convection. In this method, three uncoupled VMS treatments for the velocity, the temperature, and the concentration are introduced as the postprocessing steps at each time step, respectively. It is easy to implement because we can use the existing code. Comparing with the projection-based VMS stabilization finite element method [8], our method can save a large amount of computational cost. Stability and convergence analysis are provided; numerical tests are given to verify the effectiveness of the method. The full discretization decoupled scheme [32] or the implicit-explicit stabilization method [31] will be consider for the Darcy-Brinkman equations in double-diffusive convection in the future.

Acknowledgements This work was supported by the Natural Science Foundation of China (NSFC) under grants 11371287 and 61663043 and the Natural Science Basic Research Plan in Shaanxi Province of China under grant 2016JM5077.

References

1. Ahmed, N., Rebollo, T.C., John, V., Rubino, S.: A review of variational multiscale methods for the simulation of turbulent incompressible flows. Arch. Comput. Method. Eng. **24**, 115–164 (2017)
2. Belenli, M.A., Kaya, S., Rebholz, L.G.: An explicitly decoupled variational multiscale method for incompressible, non-isothermal flows. Comput. Methods Appl. Math. **15**, 1–20 (2015)
3. Belenli, M.A., Kaya, S., Rebholz, L.G., Wilson, N.E.: A subgrid stabilization finite element method for incompressible magnetohydrodynamics. Int. J. Comput. Math. **90**, 1506–1523 (2013)
4. Brenner, S., Scott, R.: The Mathematical Theory of Finite Element Methods. Springer, New York (1994)
5. Case, M.A., Ervin, V.J., Linke, A., Rebholz, L.G.: A connection between Scott-Vogelius and grad-div stabilized Taylor-Hood FE approximations of the Navier-Stokes equations. SIAM J. Numer. Anal. **49**, 1461–1481 (2011)
6. Chen, G., Feng, M.: Explicitly uncoupled variational multiscale for characteristic finite element methods based on the unsteady Navier-Stokes equations with high Reynolds number. Appl. Math. Model. **39**, 4202–4212 (2015)
7. Çıbık, A., Kaya, S.: A projection-based stabilized finite element method for steady-state natural convection problem. J. Math. Anal. Appl. **381**, 469–484 (2011)
8. Çıbık, A., Kaya, S.: Finite element analysis of a projection-based stabilization method for the Darcy-Brinkman equations in double-diffusive convection. Appl. Numer. Math. **64**, 35–49 (2013)
9. Cibik, A.B.: Numerical Analysis of a Projection-Based Stabilization Method for the Natural Convection Problems. Ph.D. thesis, Middle East Technical University (2011)
10. Fortin, M.: Calcul numérique des écoulements de fluides de bingham et des fluides newtoniens incompressibles par la méthode des éléments finis. Ph.D. thesis (1972)
11. Galvin, K.J.: New subgrid artificial viscosity Galerkin methods for the Navier-Stokes equations. Comput. Methods Appl. Mech. Eng. **200**, 242–250 (2011)
12. Girault, V., Raviart, P.A.: Finite Element Methods for Navier-Stokes Equations: Theory and Algorithms. Springer, New York (2012)
13. Goyeau, B., Songbe, J.P., Gobin, D.: Numerical study of double-diffusive natural convection in a porous cavity using the Darcy-Brinkman formulation. Int. J. Heat Mass Trans. **39**, 1363–1378 (1996)
14. Gresho, P.M., Lee, R.L., Chan, S.T., Sani, R.L.: Solution of the time-dependent incompressible Navier-Stokes and Boussinesq equations using the Galerkin finite element method. In: Approximation Methods for Navier-Stokes Problems, pp. 203–222. Springer, Berlin (1980)
15. Guermond, J.L., Marra, A., Quartapelle, L.: Subgrid stabilized projection method for 2D unsteady flows at high Reynolds numbers. Comput. Methods Appl. Mech. Eng. **195**, 5857–5876 (2006)
16. Gunzburger, M.: Finite Element Methods for Incompressible Viscous Flows: a Guide to Theory, Practice and Algorithms. Academic, Boston (1989)
17. Hecht, F.: New development in Freefem++. J. Numer. Math. **20**, 251–266 (2012)
18. Heywood, J.G., Rannacher, R.: Finite-element approximation of the nonstationary Navier-Stokes problem. Part IV: error analysis for second-order time discretization. SIAM J. Numer. Anal. **27**, 353–384 (1990)
19. Hughes, T.J., Mazzei, L., Jansen, K.E.: Large eddy simulation and the variational multiscale method. Comput. Vis. Sci. **3**, 47–59 (2000)
20. John, V., Kaya, S.: A finite element variational multiscale method for the Navier-Stokes equations. SIAM J. Sci. Comput. **26**, 1485–1503 (2005)
21. Kaya, S., Riviere, B.: A two-grid stabilization method for solving the steady-state Navier-Stokes equations. Numer. Methods Partial Differ. Equ. **22**, 728–743 (2006)
22. Layton, W., Röhe, L., Tran, H.: Explicitly uncoupled VMS stabilization of fluid flow. Comput. Methods Appl. Mech. Eng. **200**, 3183–3199 (2011)

23. Loewe, J., Lube, G.: A projection-based variational multiscale method for large-eddy simulation with application to non-isothermal free convection problems. Math. Models Methods Appl. Sci. **22**, 1150011 (2012)
24. Melhem, H.G.: Finite Element Approximation to Heat Transfer Through Combined Solid and Fluid Media. PhD thesis, University of Pittsburgh (1987)
25. Mojtabi, A., Charrier-Mojtabi, M.C.: Double-diffusive convection in porous media. In: Vafai, K. (ed.) Handbook of Porous Media, pp. 559–603. Marcel Dekker, New York (2000)
26. Nield, D.A., Bejan, A.: Convection in Porous Media. Springer, New York (2006)
27. Shan, L., Layton, W.J., Zheng, H.: Numerical analysis of modular VMS methods with nonlinear eddy viscosity for the Navier-Stokes equations. Int. J. Numer. Anal. Model. **10**, 943–5971 (2013)
28. Taylor, C., Hood, P.: A numerical solution of the Navier-Stokes equations using the finite element technique. Comput. Fluids **1**, 73–100 (1973)
29. Temam, R.: Navier-Stokes Equations: Theory and Numerical Analysis. North-Holland, Amsterdam (1984)
30. Trevisan, O.V., Bejan, A.: Natural convection with combined heat and mass transfer buoyancy effects in a porous medium. Int. J. Heat Mass Transf. **28**, 1597–1611 (1985)
31. Yang, Y.B., Jiang, Y.L.: Numerical analysis and computation of a type of IMEX method for the time-dependent natural convection problem. Comput. Methods Appl. Math. **16**, 321–344 (2016)
32. Yang, Y.B., Jiang, Y.L.: Analysis of two decoupled time-stepping finite element methods for incompressible fluids with microstructure. Preprint, to appear in Int. J. Comput. Math. https://doi.org/10.1080/00207160.2017.1294688
33. Zhang, Y., Wang, Z., Tang, Q.: Fully discrete subgrid stabilized finite element method for the Darcy-Drinkman equations in double-diffusion convection. In: 2015 International Conference on Advanced Mechatronic Systems (ICAMechS), pp. 413–417. IEEE (2015)